

THE UNIVERSITY OF MICHIGAN
COLLEGE OF ENGINEERING
High Altitude Engineering Laboratory
Departments of
Aerospace Engineering
Atmospheric and Oceanic Science

Final Report

LOW RESOLUTION MEASUREMENTS OF OZONE
ABSORPTIVITY IN THE 9.6 μ m REGION

F.L. Bartman

W.R. Kuhn

L.T. Loh

ORA Project 036350

under contract with:

NATIONAL AERONAUTICS AND SPACE ADMINISTRATION

CONTRACT NO. NSR 23-005-376

WASHINGTON, D.C.

administered through

OFFICE OF RESEARCH ADMINISTRATION ANN ARBOR

February 1975

TABLE OF CONTENTS

LIST OF FIGURES	v
LIST OF TABLES	ix
ABSTRACT	xi
CHAPTER	
I. INTRODUCTION	1
II. EQUIPMENT	
2.1 Ozone Generating Equipment	11
2.2 Gas Handling System and Sample Cells	15
2.3 Ozone Measuring System	18
2.4 Infrared Spectrophotometer	21
2.5 Data Handling System	22
2.6 Modifications for Low Temperature and Low Ozone Concentration	23
III. OPERATING PROCEDURES	
3.1 Preparation of Gas Sample	26
3.2 UV Measurement of Ozone	27
3.3 Infrared Spectra of Ozone	28
3.4 Data Acquisition	29
3.5 Computation and Graphical Presentation	30
IV. DATA REDUCTION AND ANALYSIS	
4.1 Introduction	31
4.2 Band Strength (ν_3)	31
4.3 Low Mass Path Measurements	32
4.4 Low Temperature Measurements	39
REFERENCES	64

LIST OF FIGURES

<u>Figure</u>	<u>Page</u>
1.1 Standard ozone profiles for lowest and highest total ozone (atm-cm) for low-, mid-, and high altitude series. From Mateer, Heath, and Krueger (1971).	2
1.2 Ozone tangent mass paths (atm-cm) for for a typical mid-latitude ozone profile.	4
2.1.1 Electric ozone generator	12
2.1.2 Circuit diagram for power supply	13
2.2.1 Gas handling system	
2.3.1 U.V. attachment on sample White cell.	20
4.2.1 ν_3 band absorptivities for small mass paths.	34
4.2.2 Transmission profiles for $9.6\mu\text{m}$ ν_3 ozone band.	35
4.2.3 Transmission profiles for $9.6\mu\text{m}$ ν_3 ozone band.	36
4.2.4 Transmission profiles for $9.6\mu\text{m}$ ν_3 ozone band.	37
4.2.5 Transmission profiles for $9.6\mu\text{m}$ ν_3 ozone band.	38
4.3.1 Percent difference between experimental absorptivity and absorptivity as calculated from Walshaw's (1957) formula (relative to Walshaw's formula). Ozone amount is determined from the 2536 \AA line.	42
4.3.2 Percent difference between experimental absorptivity and absorptivity as calculated from Walshaw's (1957) formula (relative to Walshaw's formula).	43
4.3.3 Transmission profiles for $9.6\mu\text{m}$ ν_3 ozone band.	44
4.3.4 Transmission profiles for $9.6\mu\text{m}$ ν_3 ozone band.	45
4.3.5 Transmission profiles for $9.6\mu\text{m}$ ν_3 ozone band.	46

LIST OF FIGURES (concluded)

<u>Figure</u>		<u>Page</u>
4.3.6	Transmission profiles for $9.6\mu\text{m } \nu_3$ ozone band.	47
4.3.7	Transmission profiles for $9.6\mu\text{m } \nu_3$ ozone band.	48
4.3.8	Transmission profiles for $9.6\mu\text{m } \nu_3$ ozone band.	49
4.3.9	Transmission profiles for $9.6\mu\text{m } \nu_3$ ozone band.	50
4.3.10	Transmission profiles for $9.6\mu\text{m } \nu_3$ ozone band.	51
4.3.11	Transmission profiles for $9.6\mu\text{m } \nu_3$ ozone band.	52
4.3.12	Transmission profiles for $9.6\mu\text{m } \nu_3$ ozone band.	53
4.3.13	Transmission profiles for $9.6\mu\text{m } \nu_3$ ozone band.	54
4.3.14	Transmission profiles for $9.6\mu\text{m } \nu_3$ ozone band.	55
4.4.1	Low temperature transmission profiles for $9.6\mu\text{m } \nu_3$ ozone band.	57
4.4.2	Low temperature transmission profiles for $9.6\mu\text{m } \nu_3$ ozone band.	58
4.4.3	Low temperature transmission profiles for $9.6\mu\text{m } \nu_3$ ozone band.	59
4.4.4	Low temperature transmission profiles for $9.6\mu\text{m } \nu_3$ ozone band.	60
4.4.5	Low temperature transmission profiles for $9.6\mu\text{m } \nu_3$ ozone band.	61

LIST OF TABLES

<u>Table</u>	<u>Page</u>
1.1 Values of parameters used in Walshaw's empirical formula for ozone total band absorption.	6
1.2 Ultraviolet ozone absorption coefficients ($\text{atm}^{-1}\text{cm}^{-2}$).	7
1.3 Estimates of the ν_3 band strength.	10
2.3.1 Absorption Coefficients of Ozone at 4 Wavelengths of Hg Lines.	19
4.2.1 ν_3 band absorptions used in the determination of the band intensity. Pressure range is 728-732mm Hg. Stared values refer to 2894Å u.v. line. All others refer to the 2536Å line.	33
4.3.1 ν_3 band absorption for selected pressures (mm Hg) and mass paths (atm _o cm). * and + refer to the 2967 and 2896 Å lines, respectively. All others refer to 2536 Å.	40
4.4.1 Low temperature absorptivity measurements for the ν_3 ozone band. * refers to the 2967 Å uv line, all others to the 2536 Å line.	56

ABSTRACT

Low resolution measurements of the $9.6\mu\text{m}(\nu_3)$ ozone band have been made in order to provide data for conditions of low mass paths (>0.002 atm cm) and pressures (~ 10 mm Hg), as well as low temperatures ($\sim -10^\circ\text{C}$). In addition, the band strength has been determined.

The low mass path and pressure measurements indicate that Walshaw's formula for the absorptivity is valid down to about 0.1 atm cm.

The band strength has been evaluated from the linear region of the curve of growth for sixty one absorption measurements at low mass paths and pressures of approximately 730 mm Hg. We find a band strength of $353 \text{ atm}^{-1}\text{cm}^{-2}$ (298K) with a standard error of $0.995 \text{ atm}^{-1}\text{cm}^{-2}$. This agrees closely with the result of McCaa and Shaw.

Fifteen measurements of the absorptivity were made for temperatures of approximately -10°C . The difference in transmission at room temperature and the reduced temperature as measured is shown to be consistent with theoretical estimates. There is a need to not only extend these measurements to lower temperatures, comparable to stratospheric conditions, but to improve the measurements by reducing the temperature variation ($\sim 12^\circ\text{C}$) along the absorption cell.

Computer plots of the transmission profiles which can be used for comparison with theoretical absorption studies are provided.

CHAPTER I

INTRODUCTION

The purpose of this work is to improve our knowledge of the infrared transmission properties of ozone, specifically in the $9.6\mu\text{m}$ region (ν_1 and ν_3 band) for typical pressures and mass paths encountered in the atmosphere.

Ozone, although a minor constituent of the earth's atmosphere, is very important since it shields the surface from harmful solar ultraviolet radiation and is also responsible, in large part, for the positive stratospheric lapse rate which strongly influences both the large and small scale dynamics of this region. Ozone also reacts with other minor atmospheric constituents such as the nitrogen oxides and water vapor, the latter being an important contributor - not only in the gaseous phase but also as clouds - to energy balance studies. Thus ozone is important in many environmental problems and a knowledge of its global distribution, as well as temporal and spacial variations, is necessary.

The range of atmospheric parameters over which one would like experimental ozone transmissivities can be deduced from Fig. 1.1 which shows standard ozone profiles for different latitudes. Total ozone amount is about 0.3atm cm with a variation of approximately two around this value. The concentration is a maximum in the lower stratosphere and in general decreases rather rapidly with height. Thus for vertical sensing of the atmosphere, total mass paths and pressures range from about

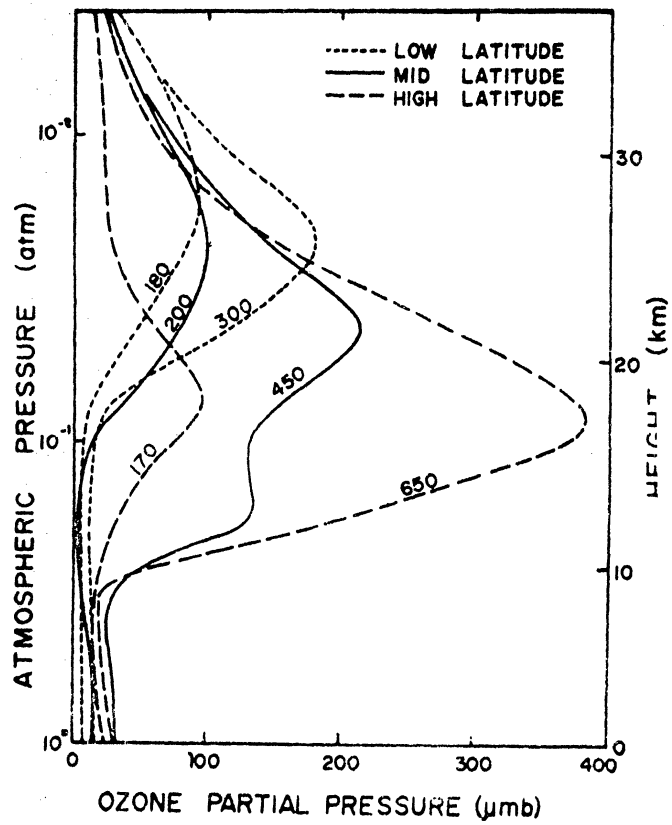


Fig. 1.1. Standard ozone profiles for lowest and highest total ozone (atm-cm) for low-, mid-, and high latitude series. From Mateer, Heath, and Krueger (1971).

0.65atm cm and 100mb to about 0.18atm cm and around 30mb. It is important to note that in this pressure range the temperature varies from about 200 to 240K depending on season and height.

For horizontal sensing of the atmosphere, mass paths and pressures can be inferred from Fig. 1.2 which shows tangent path ozone amounts for a typical mid-latitude ozone distribution. The maximum ozone amount is about 20atm cm at 200mb decreasing to 0.3atm cm at 0.8mb (50km). The variation in temperature throughout this height range is from 200-230K near the 200mb level increasing to about 260-280K near the stratopause.

Ozone is also important in stratospheric energy balance studies, and while the major contribution to the flux divergence is the absorption of solar radiation by the electronic bands, nevertheless, the $9\mu\text{m}$ region contributes about thirty percent to the total planetary cooling (Kuhn and London, 1969). For these calculations the variations in atmospheric parameters range down from about 1 atm cm (allowance being made for the diffuse approximation) and a few hundred mb pressure; the contribution to the planetary cooling is still about twenty-five percent at 60km, and for a five km thick column at this height (0.2mb) the mass path is approximately 0.001atm cm. The temperature varies from about 200K near the tropopause to about 289K at the stratopause, decreasing to about 250K at 60km.

Thus the range of interest for ozone measurements varies from a few tens of atm cm of ozone and pressures of a few hundred mb down to at least a few thousandths atm cm and

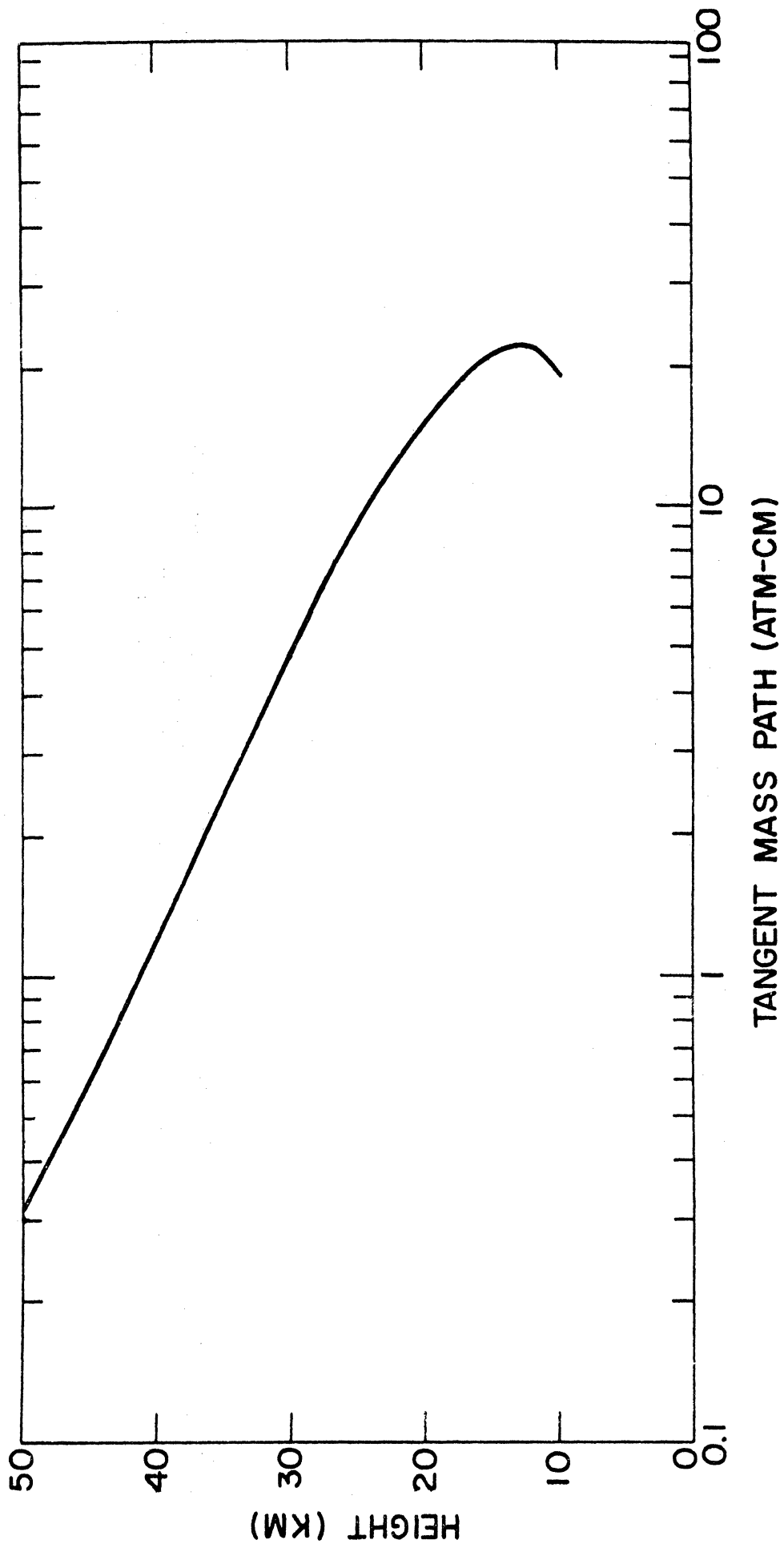


Fig. 1.2. Ozone tangent mass paths (atm-cm) for a typical mid-latitude ozone profile.

pressures to tenths of mb. The temperatures of interest are well below "room temperature", varying from about 200 to 280K. While some measurements are available they do not cover the complete range of interest and it is the purpose of this work to extend those measurements especially to lower pressures and mass paths. In addition some measurements at reduced temperatures, approximately 260K, are also analyzed.

Relatively few medium resolution $9\mu\text{m}$ ozone measurements have been made, with those of Walshaw (1957) being quoted most frequently in the literature. More recently, McCaa and Shaw (1968) measured several infrared ozone bands, among them the ν_1 and ν_3 bands; they also made a detailed comparison of their results with those of Walshaw and we shall briefly review these studies.

Walshaw's (1957) measurements of total band absorption were made with a conventional spectrometer with an equivalent slit-width of 6.5 cm^{-1} . Ozone was generated by passing an electric discharge through oxygen. The gas tested consisted of ozonized oxygen mixed with air. The results were reduced to an infinite dilution in air by assuming the ozone molecule is 1.61 times as effective in collision broadening as an "air molecule". One hundred and five measurements at room temperature were made for extreme mass paths of $.00558\text{ atm cm}$ (728 mm Hg) and 1.968 atm cm (66.9 mm Hg) and 1.795 atm cm (753 mm Hg). The systematic error in total band absorption was thought to be less than 1%. A planimeter was used to determine the absorption and

the ν_1 and ν_3 bands were separated by a "consistently applied graphical procedure," although this procedure was not explained.

Walshaw also constructed an empirical formula for the ν_3 band data which yields an r.m.s. error in total band absorption of 2.4%.

This formula has the form,

$$A_\nu = \Delta\nu [1 - 10^{-\mu f(\phi)}]$$

where $\Delta\nu = 138 \text{ cm}^{-1}$, $\mu = m\zeta$ (m), where m is the mass path in atm cm, and

$$\zeta(m) = \begin{cases} \frac{1 + .1025}{1 + 1.61m}, & m \leq 0.1 \\ -0.984 \times 10^{-0.53m}, & 0.1 \leq m \leq 0.4 \\ 0.317m^{-0.74}, & m \geq 0.4 \end{cases}$$

Also $\phi = \zeta m^{2.11}/p$ where p is in mmHg, and

$$f(\phi) = 1.185 \left(1 + 734\phi^{\frac{-1}{2}} \eta(\phi) \right), \text{ where } \eta(\phi) \text{ has the}$$

values given in the following table.

$\log_{10} \phi$	$\eta(\phi)$	$\log_{10} \phi$	$\eta(\phi)$
< -4.0	1	-3.0	0.977
-3.9	0.998	-2.9	0.979
-3.8	0.995	-2.8	0.982
-3.7	0.993	-2.7	0.989
-3.6	0.989	-2.6	1.002
-3.5	0.984	-2.5	1.016
-3.4	0.982	-2.4	1.030
-3.3	0.980	-2.3	1.045
-3.2	0.977	-2.2	1.057
-3.1	0.977	-2.1	1.069
		-2.0	1.079

Table 1.1. Values of parameters used in Walshaw's empirical formula for ozone total band absorption.

The absorption coefficients used to deduce the ozone amounts for seventy-one of the measurements were from Vigroux for 3021 and 3132 Å. Values slightly different from those of Vigroux were adopted for other wavelengths and chosen so as to minimize the difference between the measured and calculated band absorptions. Vigroux's values, and those adopted by Walshaw, as well as the presently accepted values of Hearn - are given in Table 1.2.

Wavelength (Å)	Vigroux	Walshaw	Hearn
2536	124	115.7	133.9
2894	18.2	16.0	17.2
2967			6.969
3021	3.29	3.29	3.34
3132	0.76	0.76	
3342	0.070	0.0504	.0498

Table 1.2. Ultraviolet ozone absorption coefficients ($\text{atm}^{-1} \text{cm}^{-2}$).

The absorption measurements of McCaa and Shaw (1968) utilized a Perkin Elmer Model 21 double beam spectrometer. Ozone was produced by passing oxygen through a gas discharge. Oxygen was added to the cell to bring the total pressure to that required. Forty-two total band absorptivities are presented for the ν_1 band while fifty-six are given for the ν_3 . The ν_1 and ν_3 bands were arbitrarily divided at 1070cm^{-1} , with the ν_1 extending down to 900cm^{-1} and the ν_3 up to 1250cm^{-1} . Extreme pressures and mass paths for the ν_1 band are 11.1 mmHg (.0094 atm cm) and 760 mmHg (15.4 atm cm), while for the ν_3

band the range is 15mmHg (.42atm cm) and 760mmHg (24.9atm cm); the smallest mass path is 0.08atm cm (300mmHg).

McCaa and Shaw (1968) attempted to fit their ν_1 data as well as forty-two of Walshaw's (1957) measurements to a statistical band model (with lines equally intense) with band parameters being derived from the data. They found that for some pressures and mass paths the agreement was good, although for others the agreement was poor; 40% of their measurements agree within 5% of the calculated total band absorption based on their model. The agreement is somewhat better for the ν_3 band, with 64% of their measurements falling in this 5% range. They speculate that the lack of agreement of the ν_3 band with the statistical model may occur because the R branch lines are more compact than the P branch lines, and thus a mean line spacing for the entire band is not valid.

A comparison of the estimated ν_3 band strengths is given by McCaa and Shaw (1968). We have summarized these data in Table 1.3. It is important to note that these estimates have been based, to some degree, on the data of Walshaw. Thus the various estimates are not entirely the result of different data, but rather in the use of different procedures for calculating the band strength. For example, the difference between Walshaw's estimates of the band strength and that of Goody is that Walshaw used the data in the "linear region" while Goody extrapolated Walshaw's empirical formula to low mass paths. Note that Goody's other estimate of $358\text{atm}^{-1}\text{cm}^{-2}$ which he obtained from the "linear region" agrees well with

the average of Walshaw's estimates for the 2536 Å and 2894 Å lines ($\sim 354 \text{ atm}^{-1} \text{ cm}^{-2}$). These results appear to compare favorably with those of McCaa and Shaw until one notes that McCaa and Shaw used the absorption coefficients given by Hearn while Walshaw, and presumably Goody, used Walshaw's adopted values. Indeed, when McCaa and Shaw applied the Hearn coefficients to the Walshaw data they found the band strengths to be considerably larger than their own estimates (see Table 1.3). It is also somewhat disconcerting that the band strength estimated by McCaa and Shaw from Plass's fit of Walshaw's data to the weak line approximation yields a larger band strength than McCaa and Shaw's estimate, when the same procedure is applied to the combined McCaa and Shaw, and Walshaw data.

The most recent estimate of the ν_3 band intensity has been made by Young and Bunner (1974). They determined the intensity of the $11_{9,2}-12_{9,3}$ (1027.364 cm^{-1}) line by passing laser radiation of the P(40) CO_2 line through an absorption cell containing ozone. Using results from Clough and Kneizys (1965) they were then able to calculate a band strength of $326 \pm 27 \text{ cm}^{-2} \text{ atm}^{-1}$ at 298K. Note that this estimate is appreciably lower than those of earlier studies.

The ν_1 band is much weaker than the ν_3 which overlaps it, and the band strength is difficult to determine. The only study which the authors are aware of is that of McCaa and Shaw (1968) who determined the band constants from the weak line approximation and calculated a value of $10.4 \text{ cm}^{-2} \text{ atm}^{-1}$.

<u>Author</u>	<u>Band Strength</u> ($\text{atm}^{-1}\text{cm}^{-2}$)	<u>Data</u>	<u>Method</u>	<u>u.v. line(s)</u>	<u>abs. coeff.</u>
McCaa and Shaw (1968)	350	McCaa & Shaw Walshaw	Evaluation of band constants and linear region.	2536.5 2893.6 3021.5 3341.5	Hearn
McCaa and Shaw (1968)	350	McCaa & Shaw Walshaw	Fit weak line approx. to 760 mm data.	2536.5 2893.6 3021.5 3341.5	Hearn
Walshaw (1957)	{367(425)* 340(366)}	Walshaw	Linear region	2536 2894	Walshaw
Walshaw (1954)	455	Walshaw	Linear region	2536 2894	Ny and Choong
Goody (1964)	{374 358}	Walshaw	{Extrapolation of empirical formula to small mass paths Linear region}		Walshaw
McCaa and Shaw (1968)	380	Walshaw (as plotted by Plass)	Linear region		Walshaw
Young and Bunner (1974)	326±27	(Original Clough and Kneizy)	Laser scan of ozone line	2536	Hearn Inn and Tanaka

Table 1.3. Estimates of the ν_3 band strength.

*Values in parentheses were computed by McCaa and Shaw for absorption coefficients as given by Hearn.

CHAPTER II

EQUIPMENT

2.1 OZONE GENERATING EQUIPMENT

The ozone was generated in an electric ozone generator. Its design is basically the same as that of McCaa and Shaw (1968). Fig. 2.1.1 is a side and cross sectional view of the ozone tube.

The outermost tube is a cooling jacket, made of 2.125" outside diameter copper piping, 33 inches long. Cooling water enters this jacket through the lower copper tubing and leaves through the top one. The jacket rests on the glass ozone tube on two neoprene stoppers. The ozone tube is of pyrex glass. It has three concentric tubes. The inner tube has a closed lower end. The middle one is open at the top and joins the outer one at their lower ends. A standard tapered joint 19/38 holds the inner tube concentric with the other two.

The power supply used to transform oxygen into ozone is 16kv at 60 Hz. Fig. 2.1.2 is the circuit diagram of this power supply including its metering, controlling and protecting circuits. Two power rheostats in the primary side of the transformer provide some control over the secondary voltage. Three indicator lamps, type NE-2P (General Electric Company) indicate the presence of 120V power, the condition of the fuse, and the flow of secondary current in the transformer respectively. One side of the secondary winding is the ground side of this transformer.

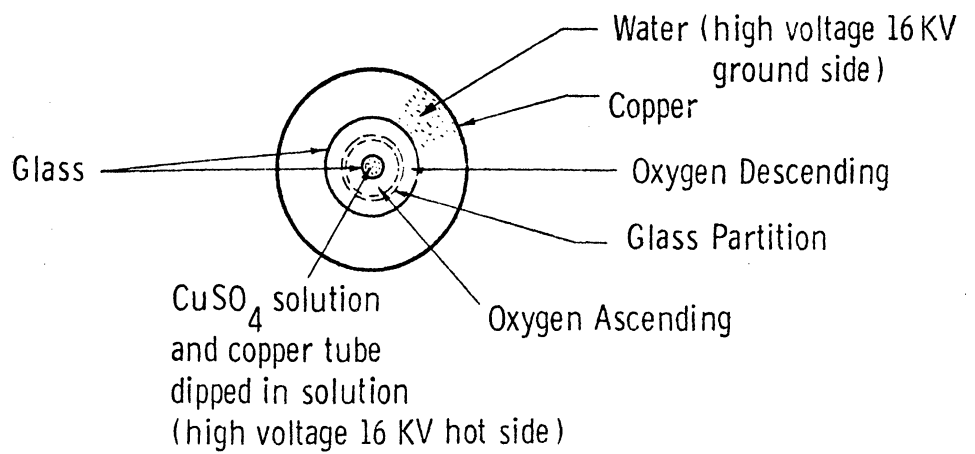
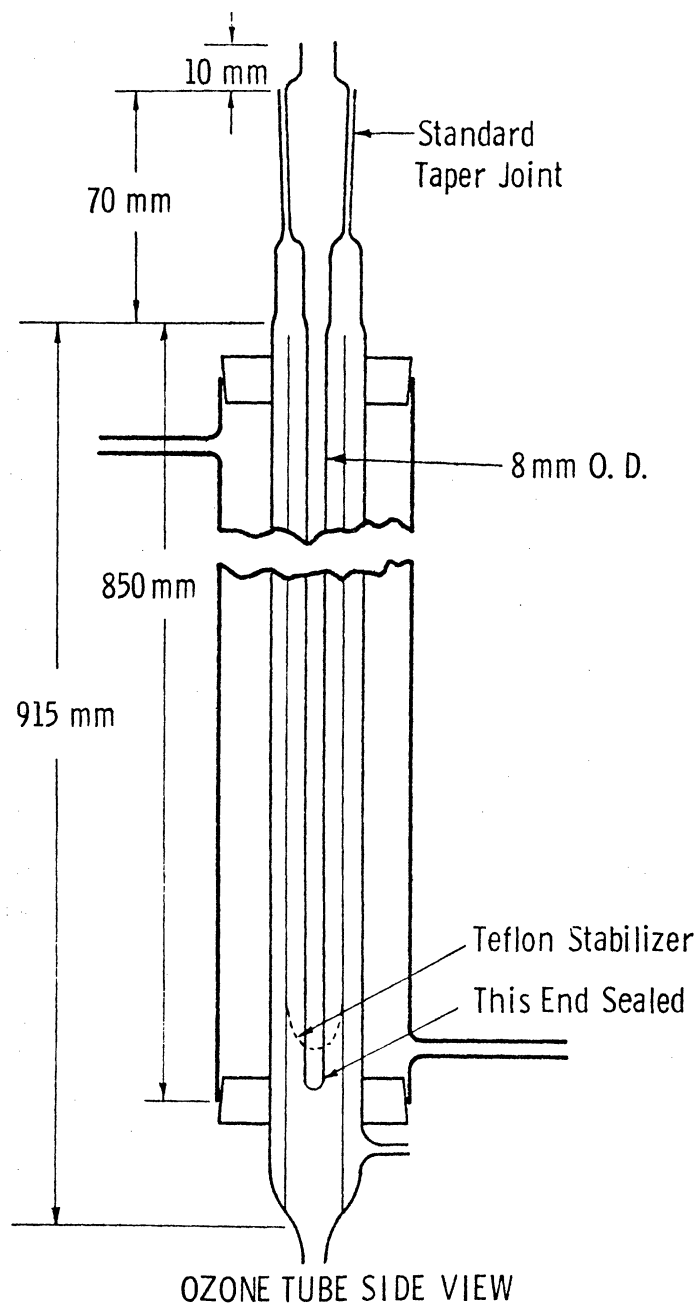


Fig. 2.1.1. Electric ozone generator

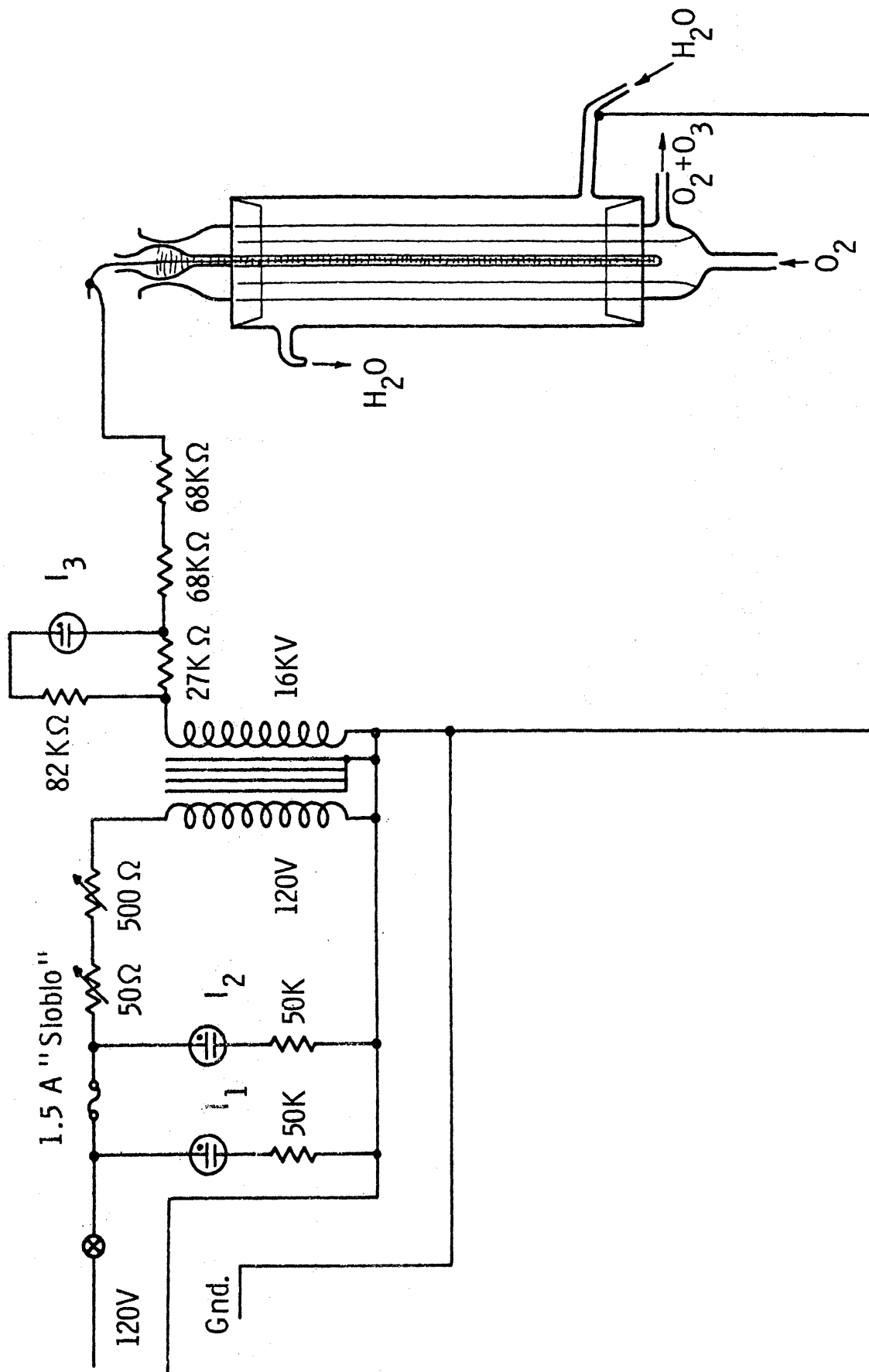


Fig. 2.1.2. Circuit diagram for power supply.

The high voltage is carried by a thin walled copper tube which extends through the innermost ozone tube, which is filled with a copper sulfate solution. This copper tube not only extends all the way through the copper sulfate solution, but also protrudes a few cm above the top end of the glass tube. It has a series of small holes drilled just below the level of the copper sulfate solution. The ground side of the high voltage goes to the copper jacket of the ozone generating tube. The cooling water has electrical conductance high enough to provide electrical contact to the outside wall of the glass ozone tube. Thus the intense AC field transforms the oxygen, coming from the bottom tubulation and flowing up and down the ozone tube into an oxygen-ozone mixture with 2-4% ozone, which leaves through the side tubulation.

The ozone generating tube rests inside a box, 8" wide, by 5" deep, by 48.5" high, of 0.5" plywood. The high voltage transformer stands on top of this box. A standoff post on the transformer serves as the connection for the hot side of the high voltage. The standoff post connects to the resistor string, which connects to the central copper tube electrode through a piece of silicon rubber insulated high voltage cable (ITT SE HV (20) 1927A(90)). All metal parts in this link have heavy coatings of silicon rubber (Dow Corning Corp. RTV #3145). Since the intense electric field around the high voltage link is a source of ozone, a plastic bag cover serves to keep most of this toxic material inside the bag.

The connection of the glass ozone tube to the 0.25" stain-

less steel piping of the gas handling system is a tygon tubing with a small piece of teflon sleeve inside each end. A coating of RTV silicon rubber on the connection helps to prevent small gas leaks.

Not shown on the circuit diagram is a clamp-on AC ammeter, model 310 meter with model 10 clamp-on adapter, of Triplet Electric Instruments Company, working through a 10-turn loop. This ammeter has the advantage of an evenly spaced scale, which makes it easier to read.

2.2 GAS HANDLING SYSTEM AND SAMPLE CELLS

Fig. 2.2.1 shows the gas handling system including a pair of 40-meter White cells on the spectrophotometer. All the pipings are stainless steel type #316. The valves are of same material and teflon. The O-rings used at various places are viton with a thin coating of Ascolube grease, Asco Manufacturing Company, Pompano Beach, Florida.

The oxygen is Airco ultrapure grade, containing at least 99.99% O₂. The factory analysis label shows, by gas chromatography, nitrogen 1.5 ppm, krypton 11.2 ppm, xenon 0.5 ppm, no other detectable impurities, and oxygen. The oxygen was used directly from the tank with no further purification step.

The flowmeter is catalog #3201-S, Cole-Parmer Instrument and Equipment Company, Chicago, Illinois. This is a shielded model with maximum pressure rating of 500 PSIG. During operation, the gas comes into contact with glass, teflon and polypropylene. The basic flowmeter uses a glass ball in a glass tube.

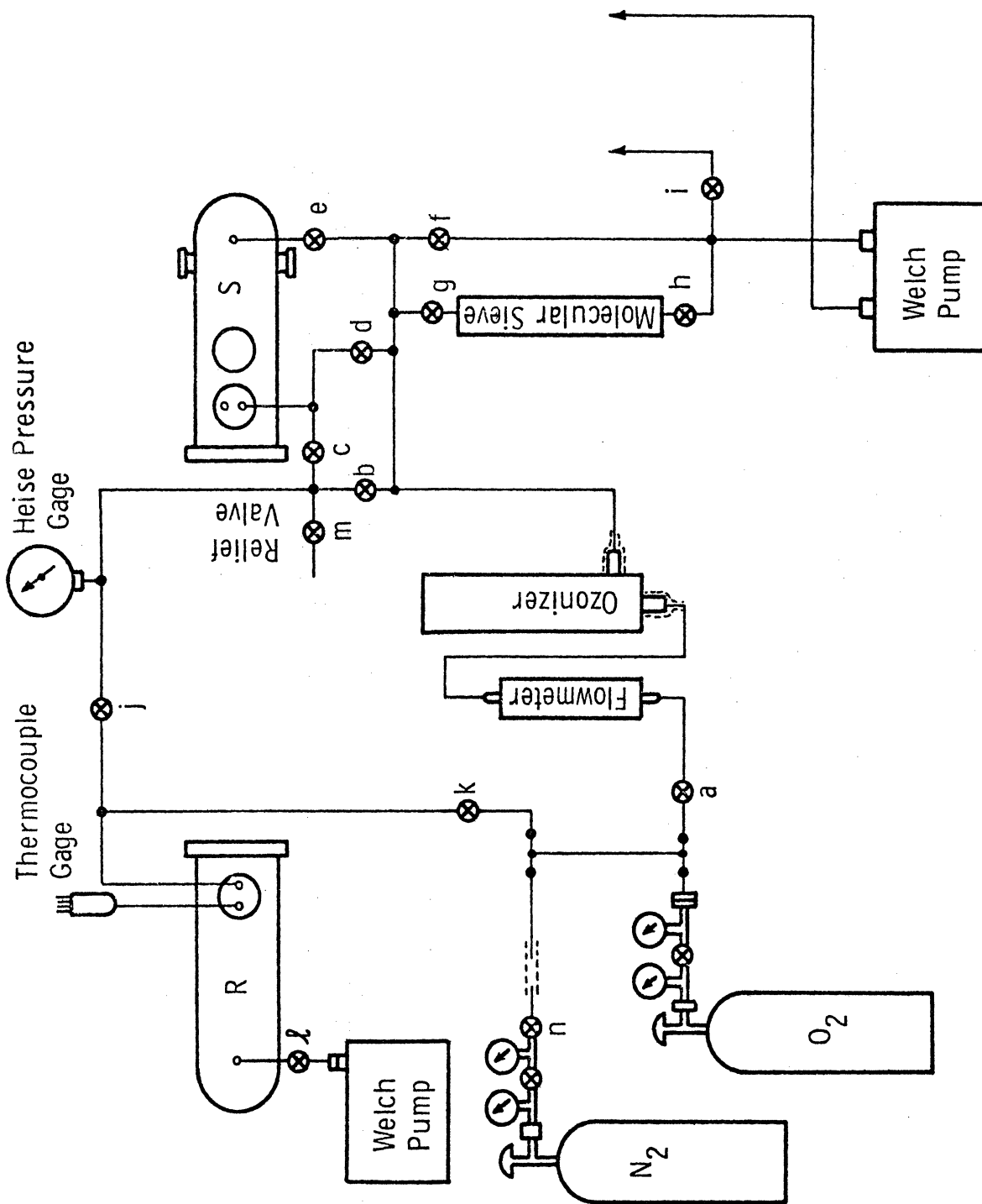


Fig. 2.2.1.1. Gas handling system.

The pressure gage is 0-100 kilopascals full scale, or 0-750mmHg. One pasal is a pressure of one newton per square meter. This is a Bourdon gage, model c, Heise Bourdon Tube Company, Newtown, Conn. The Bourdon tube and its fittings are stainless steel, type 316. It has a mirror scale and room temperature compensation.

The relief valve is type 6R-4F, Nupro Company, Cleveland Ohio. It has an adjustable range of 10-50 PSI. The valve body is stainless steel 316, the O-ring is Buna N, and valve spring is stainless steel 302. Since Buna N rubber is susceptible to ozone, the Buna N O-ring was coated with a thin layer of RTV silicone rubber.

The box marked "molecular sieves" in the diagram is type 13-X molecular sieves, in 1/16" pellets, Linde Division, Union Carbide Corporation. The container for the molecular sieves is a stainless steel pressure filtration funnel, #4280 of Gelman Instrument Company, Ann Arbor, Michigan. By pumping the used ozone sample slowly through the molecular sieves filter, the ozone will be decomposed.

The cells marked R and S in Fig. 2.2.1 are White type, made by the Perkin-Elmer Corporation, Norwalk, Conn. Each is a long path cell with optical path length adjustable from 4 to 40 meters in steps of 4 meters. The R cell was put in use with no modification. Its optical path length was set to 4 m. The S cell was modified in many ways, including the installation of fittings and windows for ultraviolet ozone monitoring system, the installation of a motor stirrer, an added port

on the cell, and the coating by spraying of teflon to the inside cell wall.

Before the coating of the sample cell with teflon, the ozone was found to disappear very rapidly. The ultraviolet ozone monitoring system is fast, but its optical path is quite different from that of the infrared. To avoid this difficulty, the ozone decomposition rate was reduced by coating the surfaces inside the S cell with teflon. The coating was applied by spraying. The material is GS-3, from RAM Chemicals, Gardena, California, in 1 pound spray can. All-together 8 cans were used, about half of them on the inside wall of the cover of the cell, and the other half on the optical parts with the mirrors and windows covered or removed. The material used for covering is thin polyethylene sheet.

2.3 OZONE MEASURING SYSTEM

On the sample cell S is an added system for monitoring the amount of ozone by the ultraviolet absorption method. The system consists of a JA45-544 mercury lamp with housing and power supply, and a JA82-410 0.25 meter Ebert monochromator (a JA83-021 photomultiplier tube housing and socket, JA26-780 amplifier/power supply, RCA 1P28 photomultiplier tube, and 2 fused silica lenses). All the JA numbers mentioned are items from Jarrel-Ash Division of Fisher Scientific Company. The fused silica lenses are ultraviolet grade from Oriel Optics Corporation, Stamford, Conn. They are planoconvex, 1.5" in diameter, and 100 mm in focal length.

The lenses serve as the transfer optics and the windows on the White cell. The distance between them is 26.8 cm. See Fig. 2.3.1 for details. The ultraviolet ray from the lamp goes through the silica lens on the top, traverses 26.8 cm through the ozone sample, goes through the silica lens on the bottom, and into the Ebert monochromator. The monochromator sends the selected line into the photomultiplier tube RCA 1P28. There are many mercury lines in the ultraviolet range useful for ozone measurement. Four of them, used in this work are shown in Table 2.3.1.

Wavelength of Hg lines λ in $\overset{\circ}{\text{A}}$	Absorption Coefficient $R(\lambda)$ in $(\text{cm NTP})^{-1}$
2536.5	133.9
2893.6	17.2
2697.3	6.969
3021.5	3.34

Table 2.3.1 Absorption Coefficients of Ozone corresponding to 4 Hg Lines.

For a given mercury line, the amount of ozone u in atmosphere cm NTP for UV is

$$u = -\frac{1}{k} \log_{10} T$$

$$= -\frac{1}{k} \log_{10} \frac{I}{I_0}$$

$$= \frac{1}{k} \log_{10} \frac{I_0}{I}$$

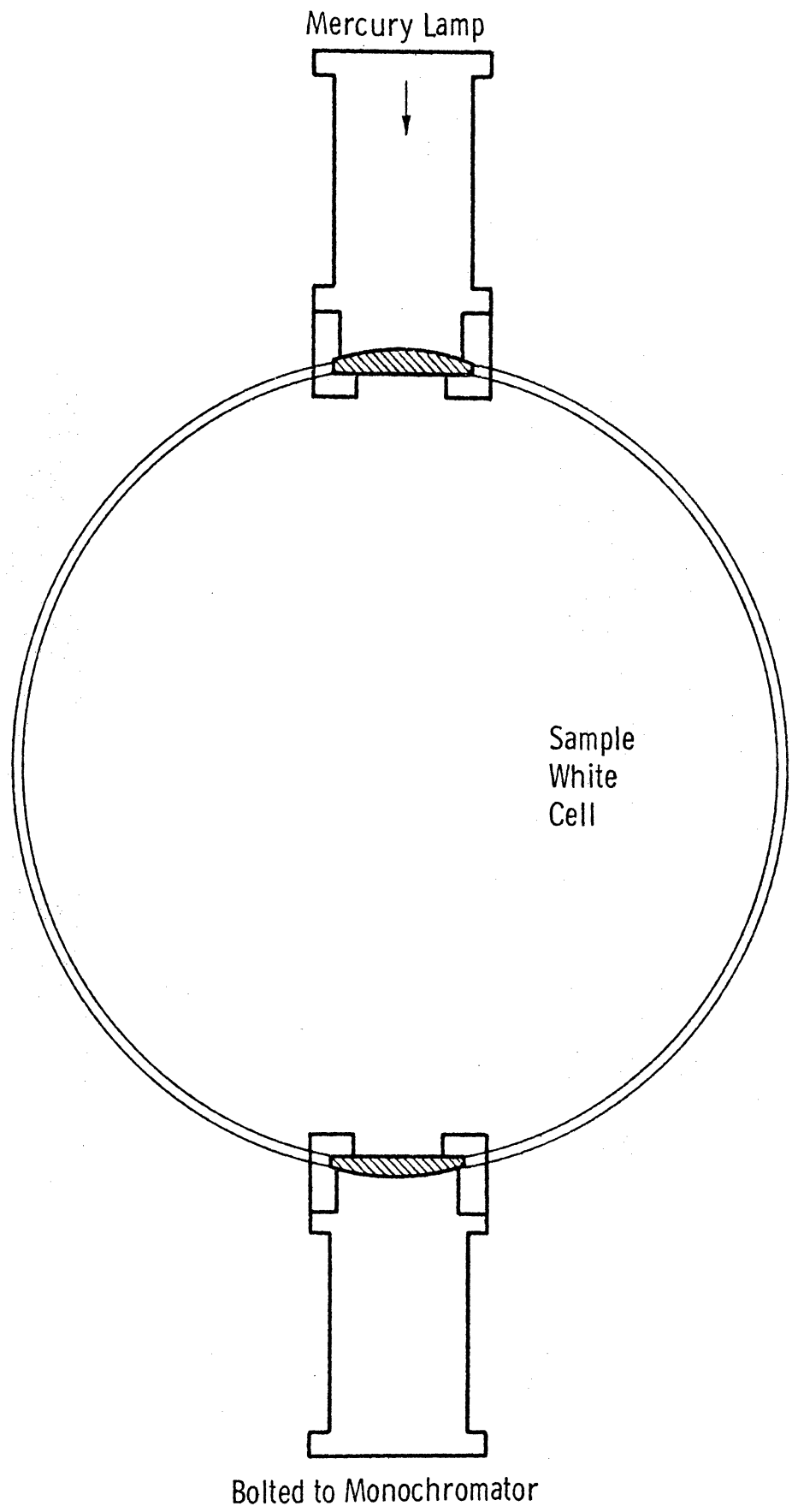


Fig. 2.3.1. U.v. attachment on sample White cell.

where k is the absorption coefficient in $(\text{cm NTP})^{-1}$. For the infrared range in the White cell, the atm cm of ozone, due to the difference of optical path length, is different from that of the uv. The factor is l/L where l is the optical path length in cm for the infrared, and L that of the uv.

A regulated power supply, model 407D of John Fluke Mfg. Co., Inc., and a microvoltammeter, model 150A of Keithley Instruments, Inc., operates the photomultiplier. The Fluke power supply has 3 voltage control potentiometers to cover the range, with the last one covering 0-0.55 V in 0.01 V per division. The voltage adjustment is fine enough even for a photomultiplier tube.

The photocurrent was also recorded continuously on a strip chart recorder. The recorder is 0-10 V full scale, Mast Development Company, model 725-3C. The output from the uv source is not constant even on a regulated 120 V power line. It takes about 2 hours to stabilize its output as indicated by the strip chart record.

2.4 INFRARED SPECTROPHOTOMETER

The infrared spectrophotometer is a model 221 of the Perkin-Elmer Corp. This is a double beam prism spectrophotometer of medium resolution, given as $0.02 \mu\text{m}$ at $12.0 \mu\text{m}$ in NaCl range. It has two prism interchanges for recording linear in transmittance and linear in wavelength, of NaCl and KBr respectively. It has a pair of longpath White cells with detachable transfer optics for each cell.

The instrument was used with only two modifications to facilitate data processing. One is the wavelength, and the other, the transmittance.

The wavelength signal is a switch closure once every 0.02 μm . This action is from a microswitch operated by a pentagon cam attached to the wavelength counter shaft. This shaft makes 1 revolution for each 0.1 μm of wavelength scan; at the same time, the pentagon cam makes 5 switching operations, or 1 operation each 0.02 μm .

The transmittance signal for the data processing is a dc voltage produced from a precision voltage source and a precision potentiometer. This potentiometer has a mechanical coupling to the shaft of the transmitting potentiometer R 3308 for the transmittance signal in the spectrophotometer. With the modification, R 3308 performs two roles. One is its electrical signal for the input of the strip chart recorder on the instrument. The other is the mechanical control of the precision potentiometer, together with the precision dc voltage source, to generate the transmittance signal for the computer.

2.5 DATA HANDLING SYSTEM

Initially the wavelength and transmittance data were processed with the aid of a PDP-8 computer. Later a Hewlett Packard data system was used (see page 30). Following is a description of the PDP-8 data handling system.

The wavelength information from the spectrophotometer is a series of switch closures, 1 for every .02 μm , or 50

closures per μm in wavelength scan. The computer senses the switch closure and issues a command signal to read the transmittance signal. The computer also issues an extra command signal after each one originated from the switch closure. The electronic clock on the system helps the timing of the command signals such that there are 100 signals evenly spaced for every $1\mu\text{m}$ of wavelength scan, with 50 of them from the cam operated microswitch, and the other 50 from the electronic clock and computer. Thus the computer system reads the spectrometer 100 times in the scan of $1\mu\text{m}$, or 1 reading for each $0.01\mu\text{m}$ of wavelength.

The transmittance signal goes into an A/D converter. At the command signal, an A/D conversion is made, and the digital datum is transferred into the stroage section of the PDP-8. To get the transmittance vs wavelength data, three seperate runs were made, one for the 100% transmittance I_{100} with nothing in the S cell, one for 0% transmittance I_0 by blocking the sample beam, and one with the sample to be investigated in the S cell I. The R cell is kept under good vacuum during all three runs. The PDP-8 data processor stores all of the information, computes, and prints the transmittance vs wavelength for each $0.01\mu\text{m}$ increment. During the printing, the system also punches out a paper tape.

2.6 MODIFICATIONS FOR LOW TEMPERATURE AND LOW OZONE CONCENTRATION.

The modifications required to measure ozone at low concentrations and temperatures consisted of lengthening of the

uv optical path, and the addition of a cooling coil onto the sample White cell with added heat insulation.

A 1 meter folded path sample cell was inserted between the White cell and the Jarrell-Ash monochromator. The uv path length was 133 cm long with the 1 meter cell in place, and 43 cm long with the path-folding by-passed. The added path length caused some loss of the uv light, therefore the photomultiplier voltage was increased for compensation. The 1 meter cell is an accessory to the Perkin-Elmer 221 spectrophotometer. Before the installation of this cell, its KBr window, and KBr window-wedge were removed, and the factory gaskets were replaced with two made of thin sheet teflon.

The temperature control modification was done by adding a cooling coil around the White cell and the added 1 meter cell. Three thermistors, (Yellow Springs Instrument Company, Yellow Spring, Ohio, type 44005 and type 44006) were mounted on the top of the White cell for temperature monitoring. About four layers of plastic heat insulation, separated by aluminum foils, were wrapped around the sample White cell and the 1 meter cell. The plastic sheet is a closed cell polyethylene foam, trade name minicel, type L-200, of Plastic Products Division, Haskon Inc., Wilmington Delaware. The cooling was done by circulation of cooled methyl alcohol with a low temperature circulator, type TK-30-DH Kryomats, Lauda Instruments Inc., Westbury, N.Y. With this circulator, a temperature of -20°C was reached. By adding a small can filled with methyl alcohol and solid

carbon dioxide into the cooling bath of this circulator, lower temperature was reached faster than the one without the solid carbon dioxide.

To keep the KBr windows at the end of this sample White cell from moisture condensation, the compartment on the spectrometer facing the window was pressurized with dry air at a flow rate of about 4 cu ft per hour. This compartment was provided with a sheet metal cover taped airtight. A small access hole was cut in this cover to facilitate the insertion and the removal of a shutter needed to make the zero percent transmittance measurement. The positive air pressure produced in this compartment helps to keep moist air from rushing into this area through the small access hole.

CHAPTER III
OPERATING PROCEDURES

3.1 PREPARATION OF GAS SAMPLE.

The preparation of the ozone sample is relatively simple. By feeding the evacuated sample White cell with oxygen, and then switching the 16kV, 60Hz Power on to the glass ozone generating tube, a 2 to 4% of ozone oxygen mixture is formed. The progress is monitored with the Heise gage for total pressure, and the uv system for the amount of ozone in atm cm in the sample White cell for the infrared. During the operation of the 16kV high voltage, the clamp-on AC ammeter operating through a 10-turn loop, in the primary circuit of the high voltage transformer, indicates the AC current used by this transformer. During the operation, the ozone generator is cooled by the circulation of water.

With enough ozone in the sample White cell, the valve between the ozone generator and the cell is closed. The mixing motor is turned on in the sequence of 10 sec on, 15 sec off, and 10 sec on. Experience has shown that this schedule is necessary and sufficient. Either the amount of ozone or the total pressure can be controlled. However, some control over both factors could be made. For example, the total pressure can be increased by addition of needed oxygen with the ozone generator off.

3.2 UV MEASUREMENT OF OZONE

The uv system monitors the amount of ozone in its optical path. From this, the amount of ozone in the infrared path can be computed. The uv source, JA 45-544 mercury lamp, housing, and power supply of the Jarrell-Ash was not very stable. It is sensitive to line voltage variation and also to room temperature. It takes several hours to stabilize its output of a given mercury line. To begin a day's work, both the uv and the IR were turned on early in the morning. The monochromator was carefully adjusted for a selected line. The 1P28 photomultiplier output is recorded on the strip chart recorder. As time goes by, the output slowly reaches stabilization.

The output current with the cell empty is the I_0 reading. To facilitate data handling, the I_0 is set to full scale on the strip chart recorder by adjusting the high voltage applied to the photomultiplier tube. This voltage is then kept unchanged for the rest of the day. With the presence of ozone in the uv path, the output current goes down. This is the I reading. The amount ozone in the uv path is then computed from I_0 and I with the formula given before. To convert into ozone in atm cm in the IR path, the value in the uv path is multiplied by the factor, path length in IR/ path length in uv.

The background reading of this uv system is quite low. Therefore, most of the time, no correction for this background was made.

3.3 INFRARED SPECTRA OF OZONE

All the infrared spectra of this study were done on a Perkin-ELmer #221 double beam spectrophotometer with long path White type cells in the NaCl prism range. This range covers 1.0-15.5 μm . However, most of the work done was for a narrow range, just wide enough to cover the particular absorption band in question. After a few trial runs covering almost the full range of the NaCl prism, the range was narrowed down to 3-6.58 μm and 7.75-11.34 μm , and then to 7.75-11.34 μm only.

For low concentration studies, the uv absorption path was lengthened from 26.8 to 133 cm. The lowest amount of ozone studied was 0.0022 atm-cm. With a long uv path of 133 cm, and a Hg line 2536 \AA the uv measurement of very low ozone concentration presented no problems.

The total pressure of ozone and oxygen ranged from a fraction of an atmosphere to less than 10 millimeters of Hg. Most of the low total pressure measurements also corresponded to a low amount of ozone.

Until the installation of the temperature control on the sample White cell, all the measurements were done with both the sample cell and the reference cell at room temperature. With the temperature control, a lower temperature of about 0⁰C was used.

During a working day, the IR spectrophotometer was turned on early in the morning for stabilization. At the same time the cell were pumped, and the uv system was turned on.

After around 1:00 PM, the 100% line of the ozone was taken with both the sample and reference cells evacuated. Next, the 0% line was taken by blocking the sample beam. Then the sample cell was filled with ozone and oxygen, and the absorption spectrum was taken. Each time, the spectrophotometer was made to scan the same wavelength interval. The ozone spectrum step was repeated several times during the day using several different values of ozone and oxygen. Only 1 set of 100% line and 0% line was taken.

A scan from 7.75-11.34 μm required about 9 minutes and 10 seconds. With 100 readings per μm , the wavelength scan rate is about 152 seconds per μm , or 1.52 sec per reading.

An analog record was produced on the spectrophotometer during each scan. This is a record showing the ratio of sample beam and reference beam vs linear wavelength.

3.4 DATA ACQUISITION

The Perkin-Elmer 221 spectrophotometer produces a record of IR absorption spectrum in the form of % transmittance vs wavelength in μm . The % transmittance scale is linear, and so is that of the wavelength. The repeatability of the plots was good, however the I_{100} line did not always exactly coincide with the printed 100% line on the record chart. Most of the time, all the spectra of a day were recorded on the same chart. To help to indentify one spectrum from another, recording pens different in ink color were used.

The data were also recorded on a PDP-8 computer system. For each scan of the wavelength, 100 readings were digitized and stored in the computer for each μm , in 0.01 μm intervals. The computer computes and prints the % of transmittance of each reading for each 0.01 μm , using the I_{100} and I_0 data stored earlier. Simultaneously, the computer system punches a paper tape for future machine processing.

As an alternative to the PDP-8, a Hewlett-Packard data system was installed in October of 1972. Data were processed once for each 0.01 μm of wavelength scan. Each reading is the time average of the analog signal for exactly 1 second. The digital voltmeter of this system displays the averaged voltage value, and also prints the number with the mechanical printer.

3.5 COMPUTATION AND GRAPHICAL PRESENTATION

The data from the PDP-8 computer are % of transmittance vs wavelength in the form of a tabulated teleprinter copy, and also in punched tape. From these, a set of IBM punched cards were prepared. The Hewlett-Packard data acquisition system provides printed data in I_{100} vs wavelength, and also for that of I_0 and I . From these, sets of IBM cards were punched. The IBM cards were further processed into cards in terms of % transmittance vs wavelength.

The IBM cards of % transmittance vs wavelength are used to produce the calcomp plots of ozone spectra. The same cards were used to compute the absorptivities of ozone for analysis and are detailed in Chapter IV.

CHAPTER IV

DATA REDUCTION AND ANALYSIS

4.1 INTRODUCTION

Absorption data were obtained over the spectral region from 7.76 μm to 11.35 μm at intervals of 0.01 μm . Data were recorded on paper tape and later punched on cards; the analysis was carried out on the IBM 360 computer.

The 0 and 100% transmission levels were determined as the average of the readings from 7.76 μm to 8.00 μm and from 11.00 to 11.35 μm . These spectral regions are far enough removed from the band center so that no absorption takes place for the mass paths and pressures used in this study. As seen from the computer plots of the transmission, the noise level is generally less than 1%.

The 9.6 μm band absorptivity was calculated from 9.35 μm to 11.00 μm . Although the total absorptivity from 8.00 μm to 11.00 μm is given, no attempt to infer the 9.1 μm absorptivity was made, since for the low mass paths used in this study the band absorptivity is very near the noise level.

4.2 BAND STRENGTH (ν_3)

A set of sixty one absorption measurements were made for pressures of approximately 730 mmHg and mass paths of 0.002 to 0.09atm cm (see Table 4.2.1) These data are shown in Fig. 4.2.1 along with those of Walshaw(1957); the pressure of approximately 730 mmHg was chosen so as to be in agreement with his study.

Ten of our measurements used the 2894 Å Hg line to monitor the ozone amount while the 2536 Å line was used for the other measurements. Walshaw also used the 2894 Å (8) and 2536 Å (3) lines; his ozone amounts have been modified for the Hearn absorption coefficients.

The band strength can be determined from Fig. 4.2.1., since the absorption is proportional to the mass path for these low absorber concentrations (weak line approximation) and the strength is given by the slope of the line representing these data. A close inspection of these data indicates the weak line approximation is valid at least to 0.05 atm cm, and a least-squares fit of our 54 data points yields a band strength of $353 \text{ atm}^{-1} \text{ cm}^{-2}$ (298⁰ K) with a standard error of $0.995 \text{ atm}^{-1} \text{ cm}^{-2}$. A least squares fit of our data over mass paths less than 0.025 atm cm (33 data points) the range of mass paths used by Walshaw, gives a band strength of $350 \text{ atm}^{-1} \text{ cm}^{-2}$ with a standard error of 0.269 cm^{-1} . Thus these results are in excellent agreement with the value of $350_{-10}^{+40} \text{ cm}^{-2} \text{ atm}^{-1}$ determined by McCaa and Shaw (1968).

Selected computer plots of the transmission for the measurements in Table 4.2.1 are given in Figs. 4.2.2 to 4.2.5.

4.3 LOW MASS PATH MEASUREMENTS

Seventy-seven measurements of the absorptivity of the 9.6 μ band were made for low mass paths, generally less than 0.07 atm cm and pressures of approximately 10 mmHg. The ozone amount was determined from the 2536 Å line. A few measurements were also made for somewhat larger mass paths, up to

TABLE 4.2.1

ν_3 band absorptions used in the determination of the band intensity. Pressure range is 728-732mm Hg. Stared values refer to 2894Å u.v. line. All others refer to the 2536Å line.

Mass path (atm cm)	band absorption (cm^{-1})	Mass path (atm cm)	band absorption (cm^{-1})	Mass path (atm cm)	band absorption (cm^{-1})
.0025	1.04	.0111	3.97	.0316	10.65
.0027	2.85	.0111	4.04	.0330	15.45
.0040	2.54	.0113	5.53	.0346	15.66
.0043	2.33	.0114	5.92	.0382	12.94
.0045	1.21	.0118	5.69	.0394	14.54
.0053	1.92	.0118	3.39	.0400	13.96
.0058	2.07	.0121	5.99	.0417	14.64*
.0064	3.01	.0151	5.13	.0436	15.07*
.0077	2.86	.0164	6.66	.0445	15.41*
.0078	2.45	.0177	6.78	.0465	15.54*
.0081	2.66	.0198	7.80	.0530	18.39
.0082	2.33	.0203	7.82	.0570	18.03*
.0082	2.39	.0212	9.29	.0590	19.42*
.0082	3.77	.0234	9.70	.0614	19.82*
.0086	3.25	.0234	10.15	.0646	20.64
.0090	2.98	.0242	9.17	.0665	20.41
.0094	2.88	.0300	11.07	.0680	22.33*
.0104	4.98	.0304	11.54	.0803	25.79
.0104	4.86	.0311	10.72	.0830	25.49*
.0110	3.44	.0315	12.07	.0866	26.35*
.0110	3.77				

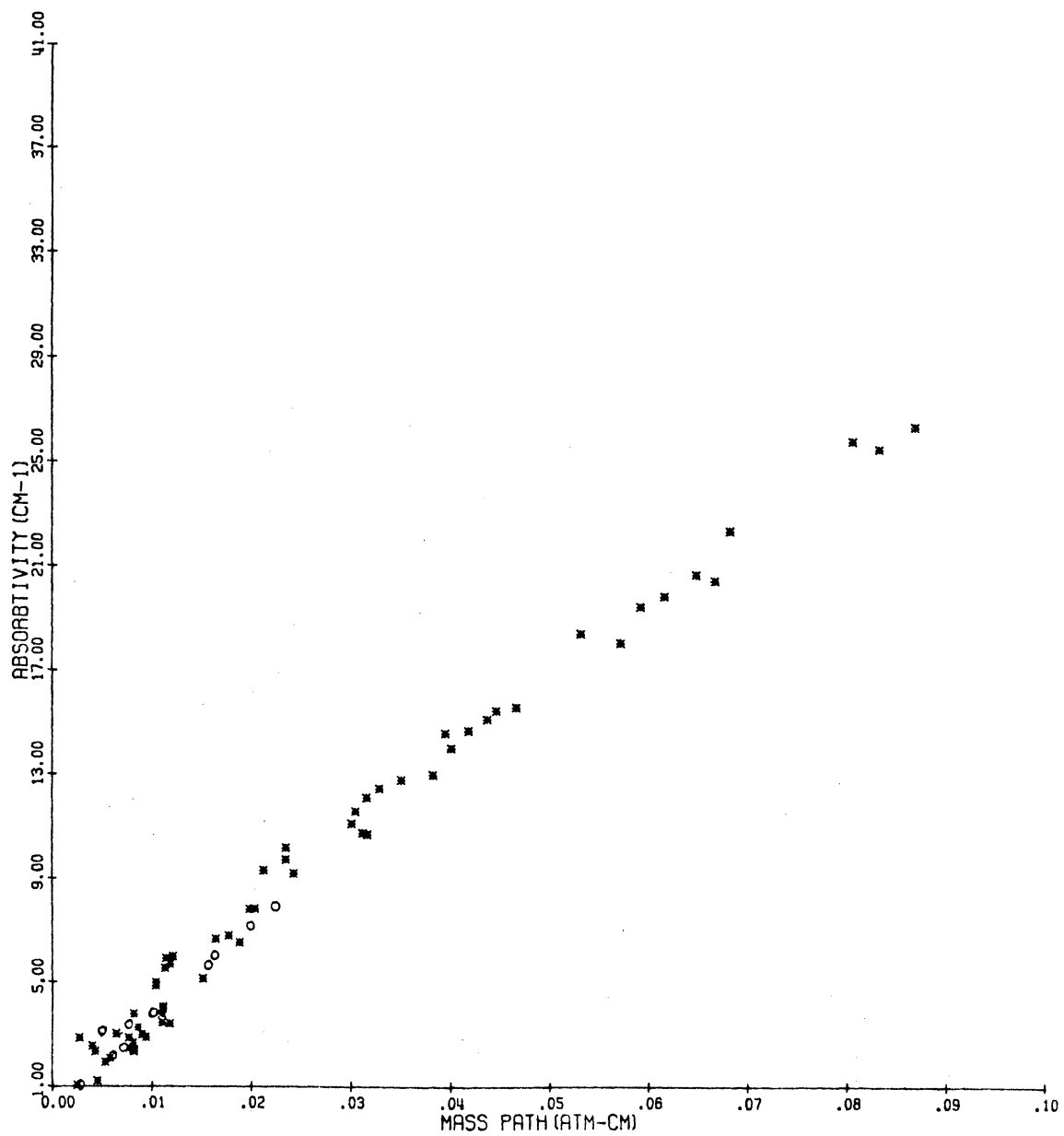


Fig. 4.2.1. ν_3 band absorptivities for small mass paths.

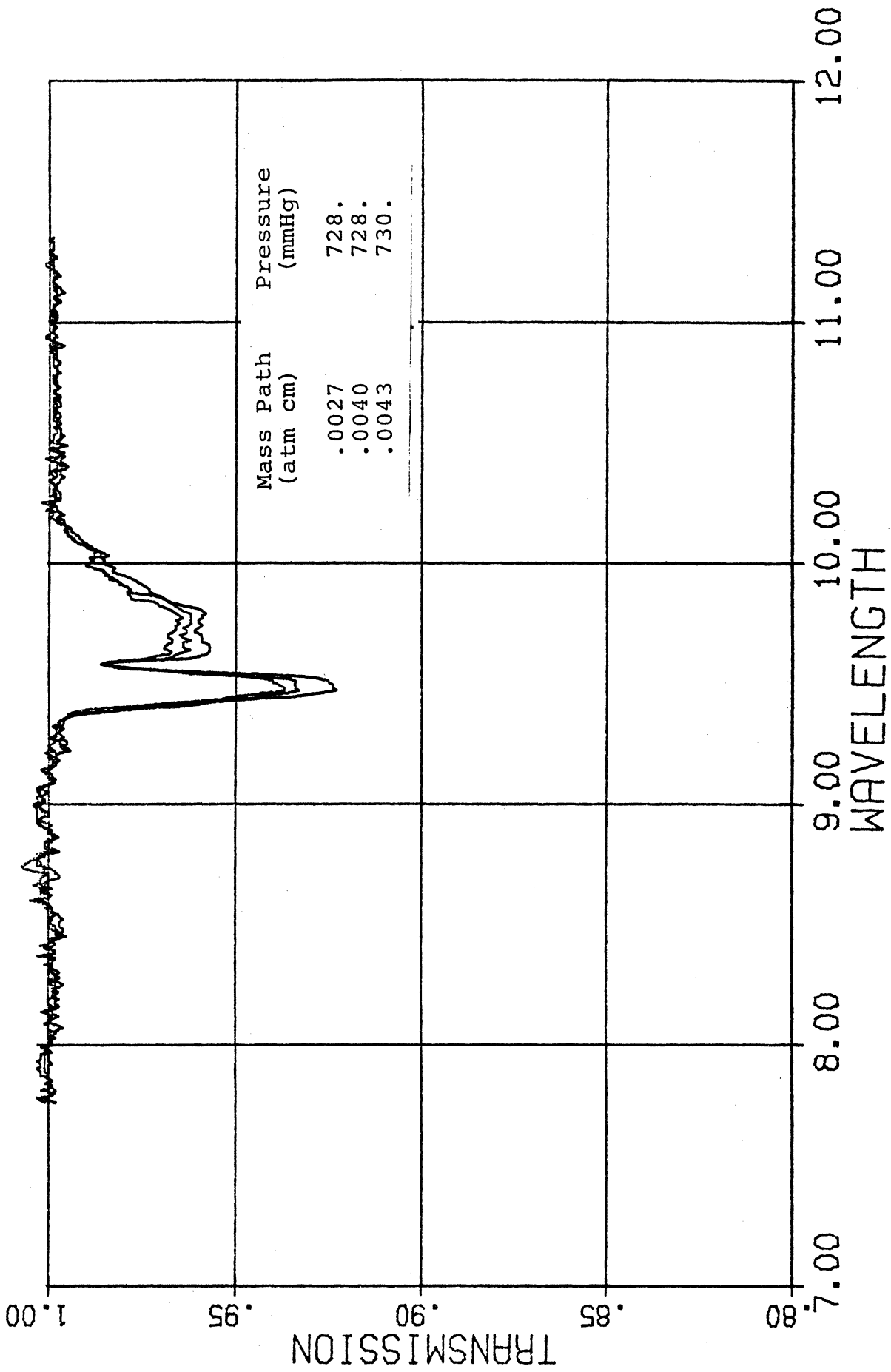


Fig. 4.2.2. Transmission profiles for 9.6 μ m ν_3 ozone band.

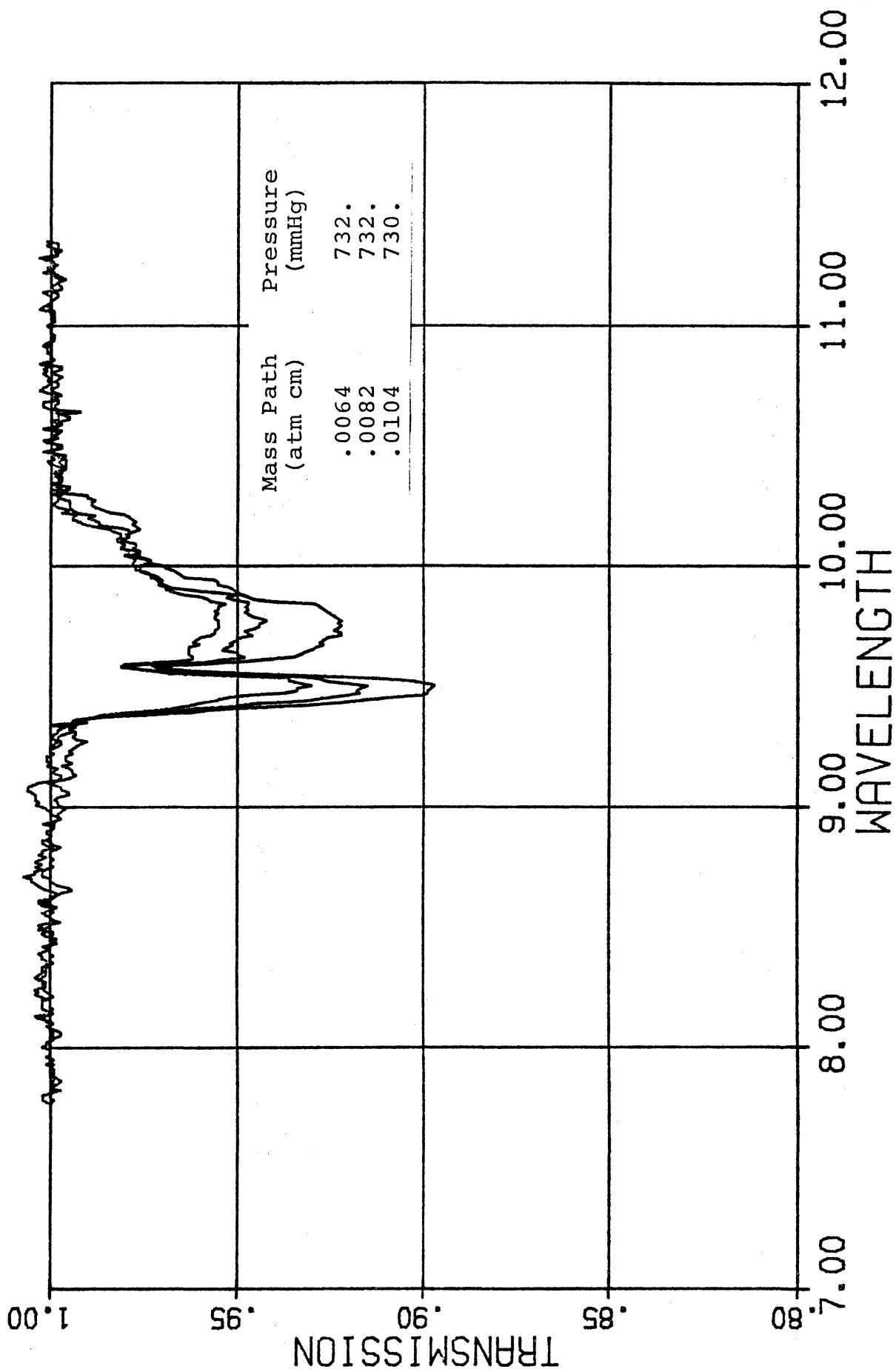
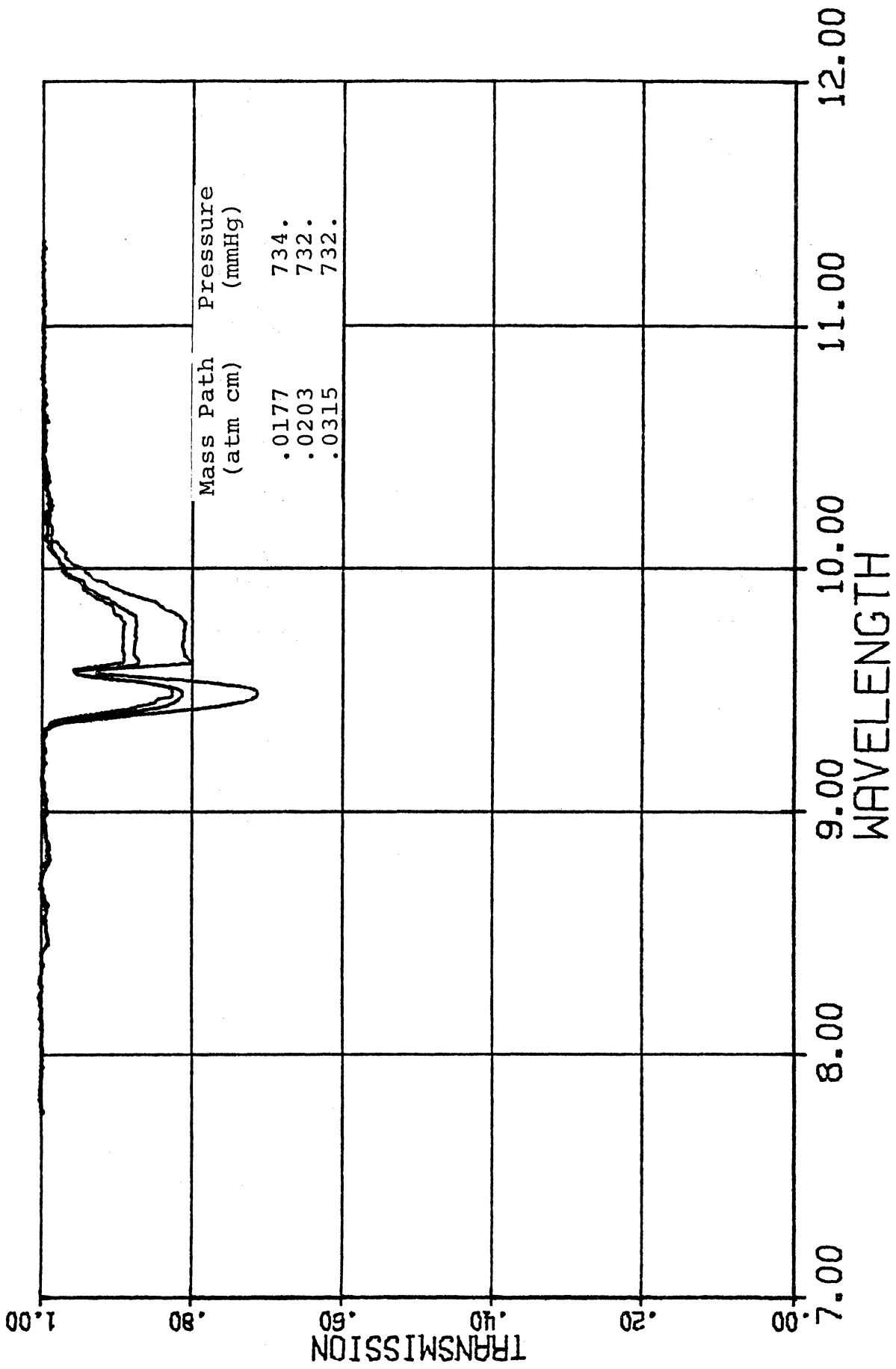


Fig. 4.2.3. Transmission profiles for $9.6\mu\text{m } \nu_3$ ozone band.



4.2.4 Transmission profiles for 9.6 μ m ν_3 ozone band.

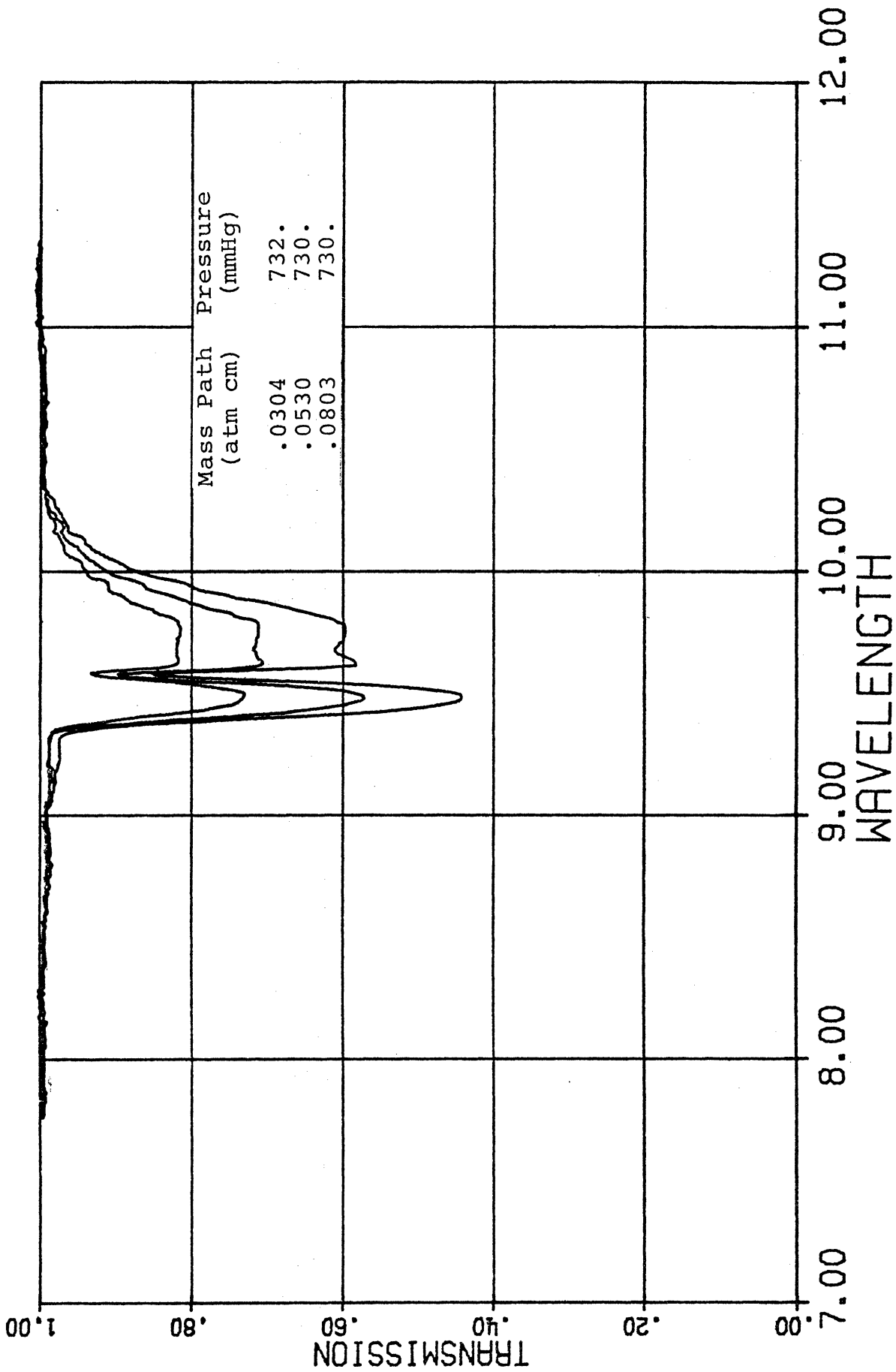


Fig. 4.2.5. Transmission profiles for $9.6\mu\text{m } \nu_3$ ozone band.

approximately 1 atm-cm; for these measurements the 2967 and 2896 $\overset{0}{\text{A}}$ lines were used. These data are shown in Table 4.3.1.

A comparison of these absorptivities with those as calculated from Walshaw's empirical formula is shown in Figs. 4.3.1 and 4.3.2. For mass paths larger than about 0.1atm-cm, Walshaw's formula agrees within $\pm 5\%$. However, Walshaw (1957) indicated that his formula is in error for pressures less than about 10 mmHg since he has not considered Doppler Broadening.¹ This is clearly shown in Fig. 4.3.1, where for mass paths less than about 0.08atm-cm, the absorptivity is some 20-40% larger than predicted by the formula. Also for these low pressures, the lines are essentially non-overlapping, which provides greater absorption than in the overlapping case.

Computer plots of the transmission for the above measurements are given in Figs. 4.3.3 to 4.3.14. These data are available on cards, with transmissions given for each 0.01 μm .

4.4 LOW TEMPERATURE MEASUREMENTS

Several measurements of the ν_3 absorptivities at reduced temperatures were made and are given in Table 4.4.1. The corresponding computer plots are shown in Figs. 4.4.1 to 4.4.5.

A major difficulty with these measurements is that a temperature gradient existed along the absorption cell; the temperature at the cell neck was near 0 $^{\circ}\text{C}$, approximately -12 $^{\circ}\text{C}$ at the opposite end of the cell, and the midpoint of the cell had the lowest temperature of approximately -15 $^{\circ}\text{C}$. These measurements are discussed in Chapter II.

¹For a pressure of 10 mmHg, the Doppler and Lorentz half widths for the 9.6 μ lines are approximately equal.

TABLE 4.3.1

ν_3 band absorption for selected pressures (mm Hg) and mass paths (atm cm). * and + refer to the 2967 and 2896 Å lines respectively. All others refer to 2536 Å.

Mass path	Pressure	Absorption	Mass path	Pressure	Absorption
.0022	4.1	0.78	.0115	4.5	3.37
.0023	3.9	0.80	.0112	5.3	3.22
.0029	3.3	1.06	.0121	4.5	3.51
.0031	3.3	1.13	.0124	3.8	2.78
.0043	3.3	1.47	.0141	5.3	3.70
.0043	1.5	1.36	.0148	5.3	3.90
.0046	1.5	1.38	.0182	10.1	4.94
.0047	3.3	1.55	.0187	10.1	5.00
.0063	4.1	2.03	.0222	5.9	5.20
.0071	4.1	2.10	.0234	5.9	5.39
.0071	4.7	2.28	.0250	9.0	6.14
.0075	4.7	2.33	.0258	9.0	6.35
.0078	7.9	2.64	.0268	6.3	5.80
.0080	7.9	2.72	.0275	10.2	6.57
.0087	3.8	2.44	.0283	6.3	6.05
.0092	7.5	3.05	.0288	10.2	6.48
.0095	7.5	2.79	.030	9.8	6.94
.0100	3.8	2.56	.0308	9.8	7.06
.0106	5.3	2.87	.032	7.2	6.55
.0110	3.8	2.65	.035	7.2	6.48

TABLE 4.3.1 (concluded)

Mass path	Pressure	Absorption	Mass path	Pressure	Absorption
.0365	10.5	8.15	.067	10.6	11.55
.0375	9.0	7.57	.168	15.4	19.88
.0375	10.3	8.14	.177	15.2	20.33
.039	10.8	8.65	.177	9.5	18.10 *
.039	10.8	8.55	.180	9.5	18.37 *
.0395	9.1	7.88	.185	15.1	20.55
.0414	9.1	7.98	.335	36.4	38.18 *
.0402	6.4	7.20	.361	36.5	39.50 *
.0417	6.4	7.34	.381	36.5	40.68 *
.0435	6.8	7.35	.398	36.5	41.39 *
.0450	6.8	7.52	.409	39.9	42.58 *
.0466	7.9	8.30	.414	39.9	42.70 *
.0470	6.8	7.60	.592	31.3	43.34 +
.0490	12.2	9.94	.630	31.0	44.46 +
.0492	7.9	8.67	.680	30.5	47.08 +
.051	13.5	10.49	.906	47.8	55.19 +
.051	13.5	10.55	.937	47.7	55.77 +
.051	12.2	10.14	.966	47.6	56.29 +
.065	10.6	11.48			

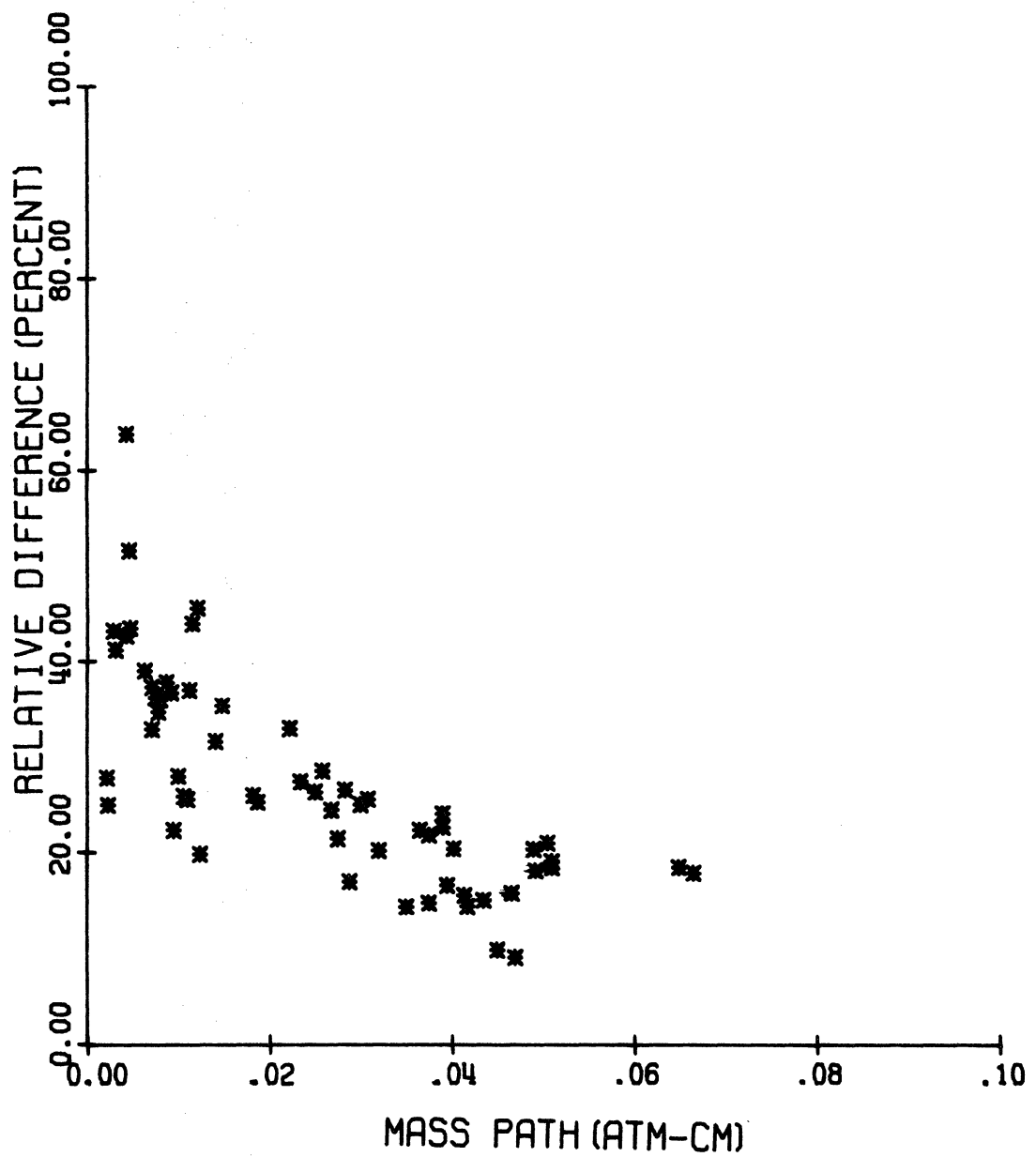


Fig. 4.3.1. Percent difference between experimental absorptivity and absorptivity as calculated from Walshaw's (1957) formula (relative to Walshaw's formula). Ozone amount is determined from the 2536 Å line.

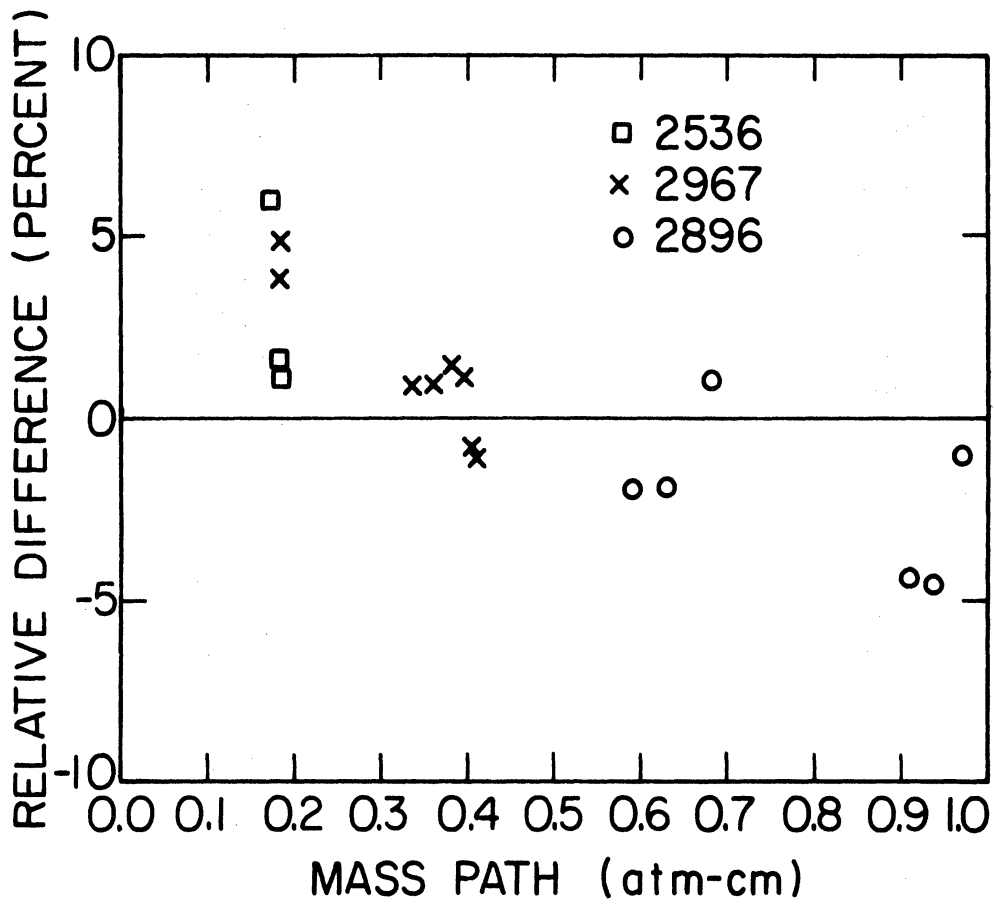


Fig. 4.3.2. Percent difference between experimental absorptivity and absorptivity as calculated from Walshaw's (1957) formula (relative to Walshaw's formula).

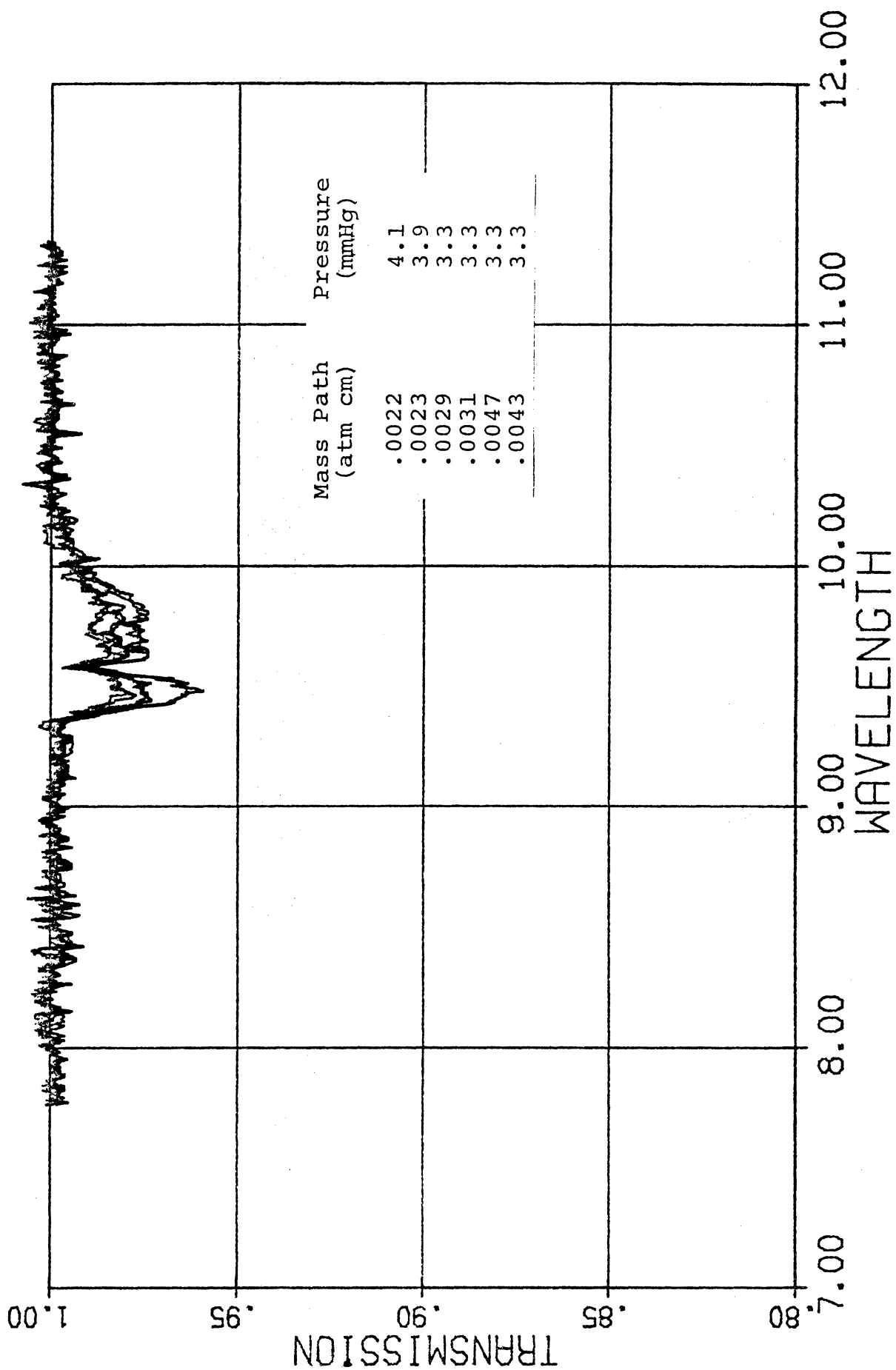


Fig. 4.3.3 Transmission profiles for $9.6\mu\text{m } \nu_3$ ozone band.

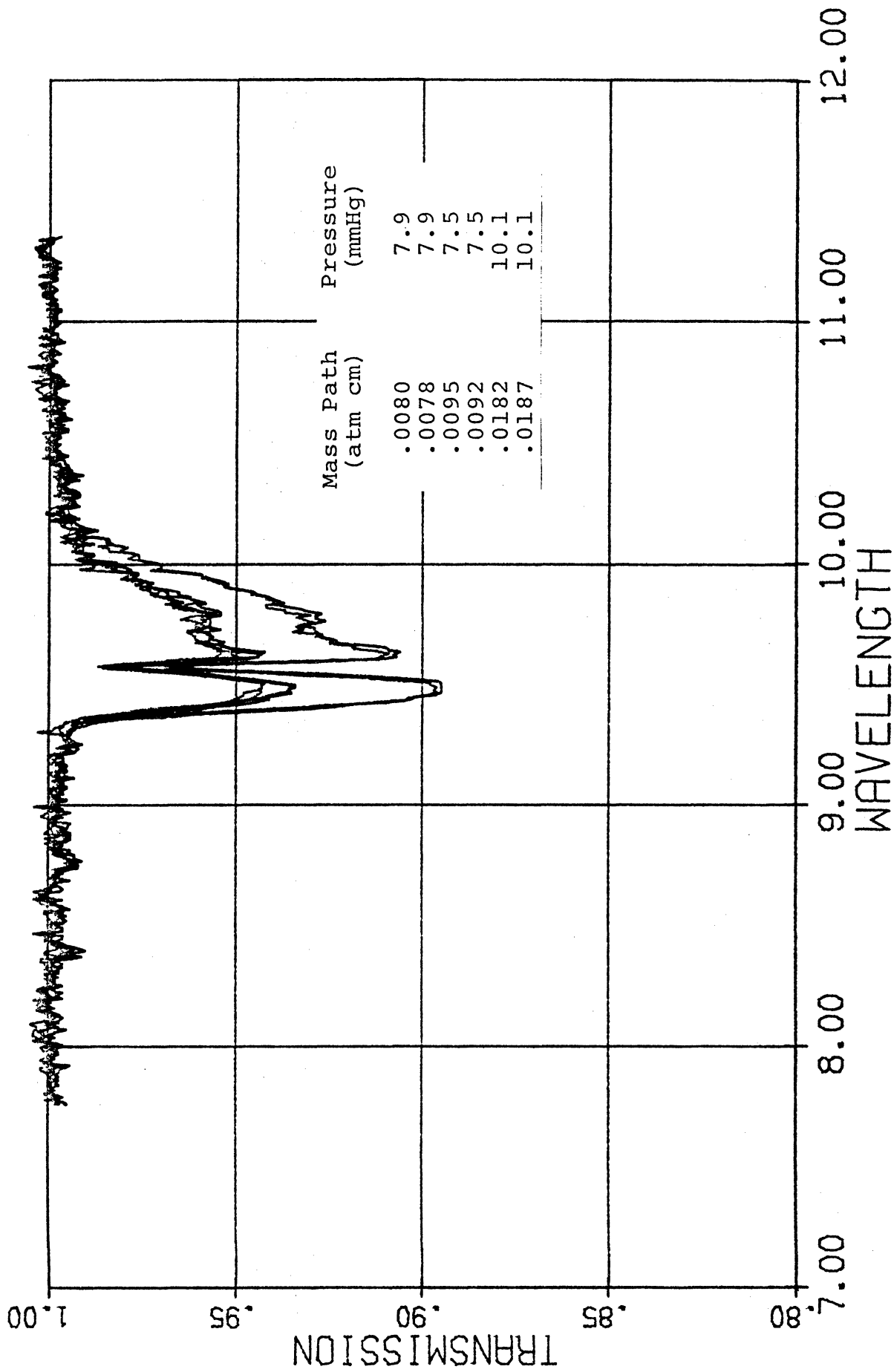


Fig. 4.3.4. Transmission profiles for $9.6\mu\text{m } \nu_3$ ozone band.

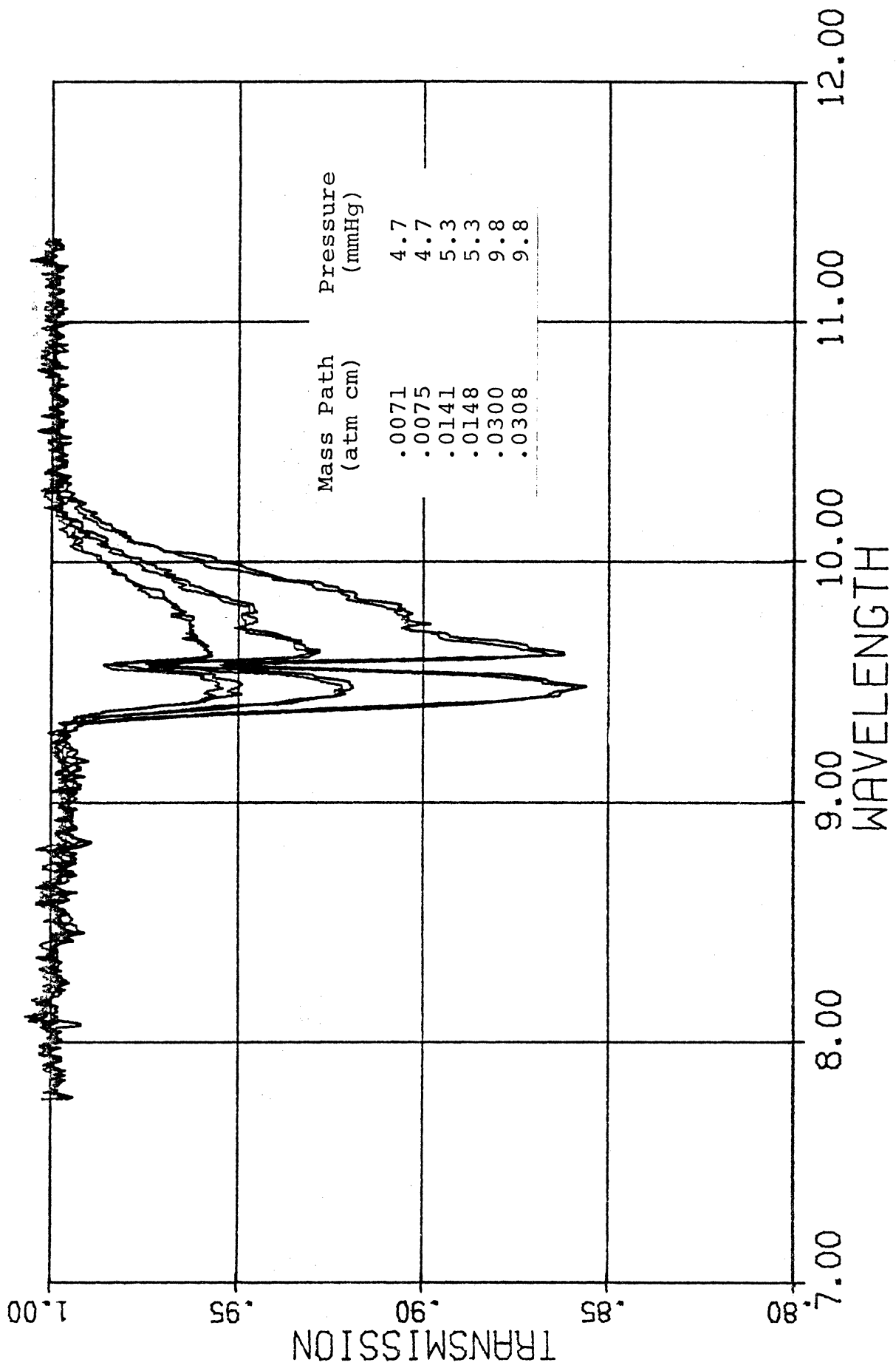


Fig. 4.3.5. Transmission profiles for $9.6\mu\text{m } \nu_3$ ozone band.

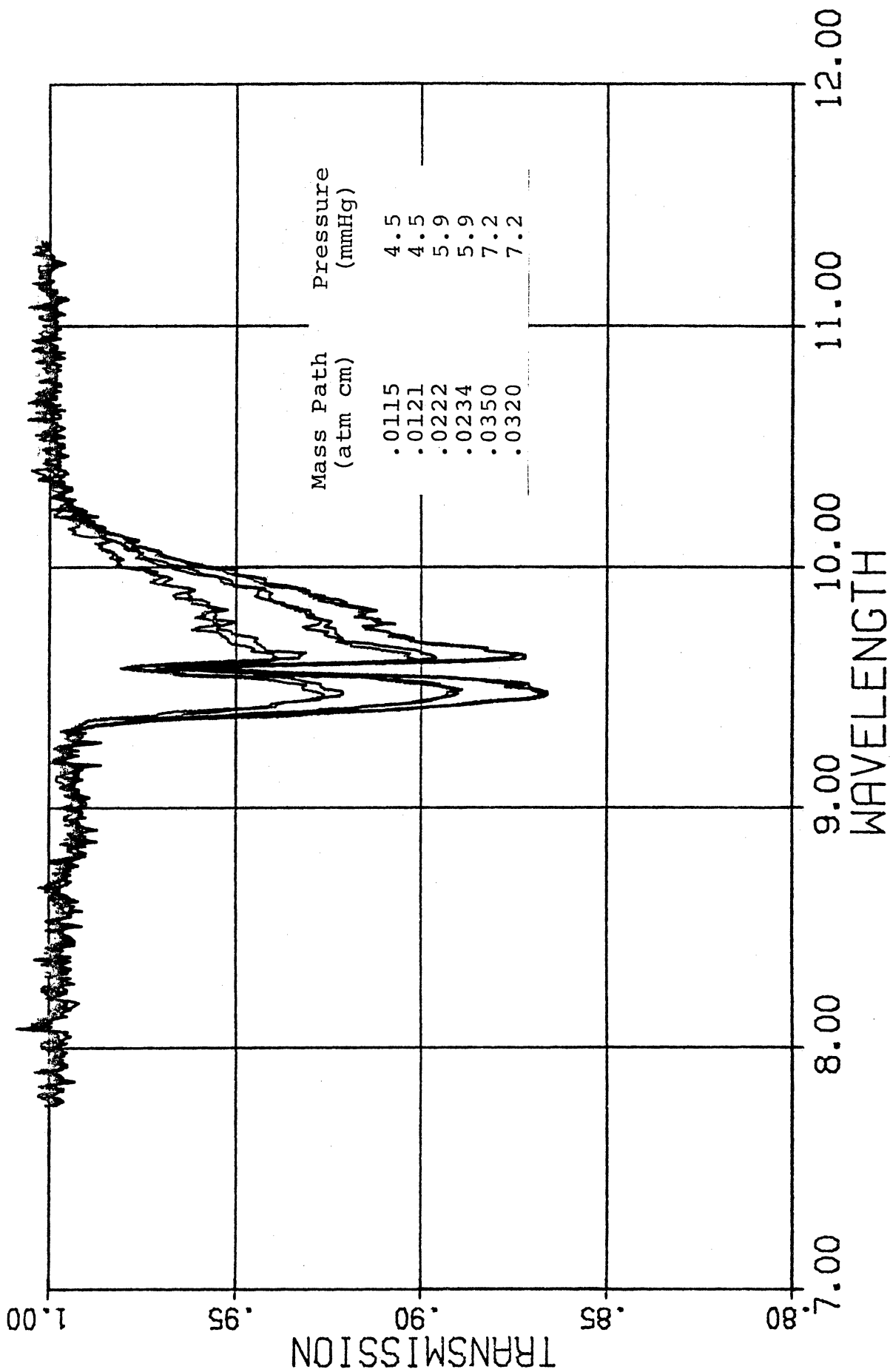


Fig. 4.3.6. Transmission profiles for $9.6\mu\text{m } \nu_3$ ozone band.

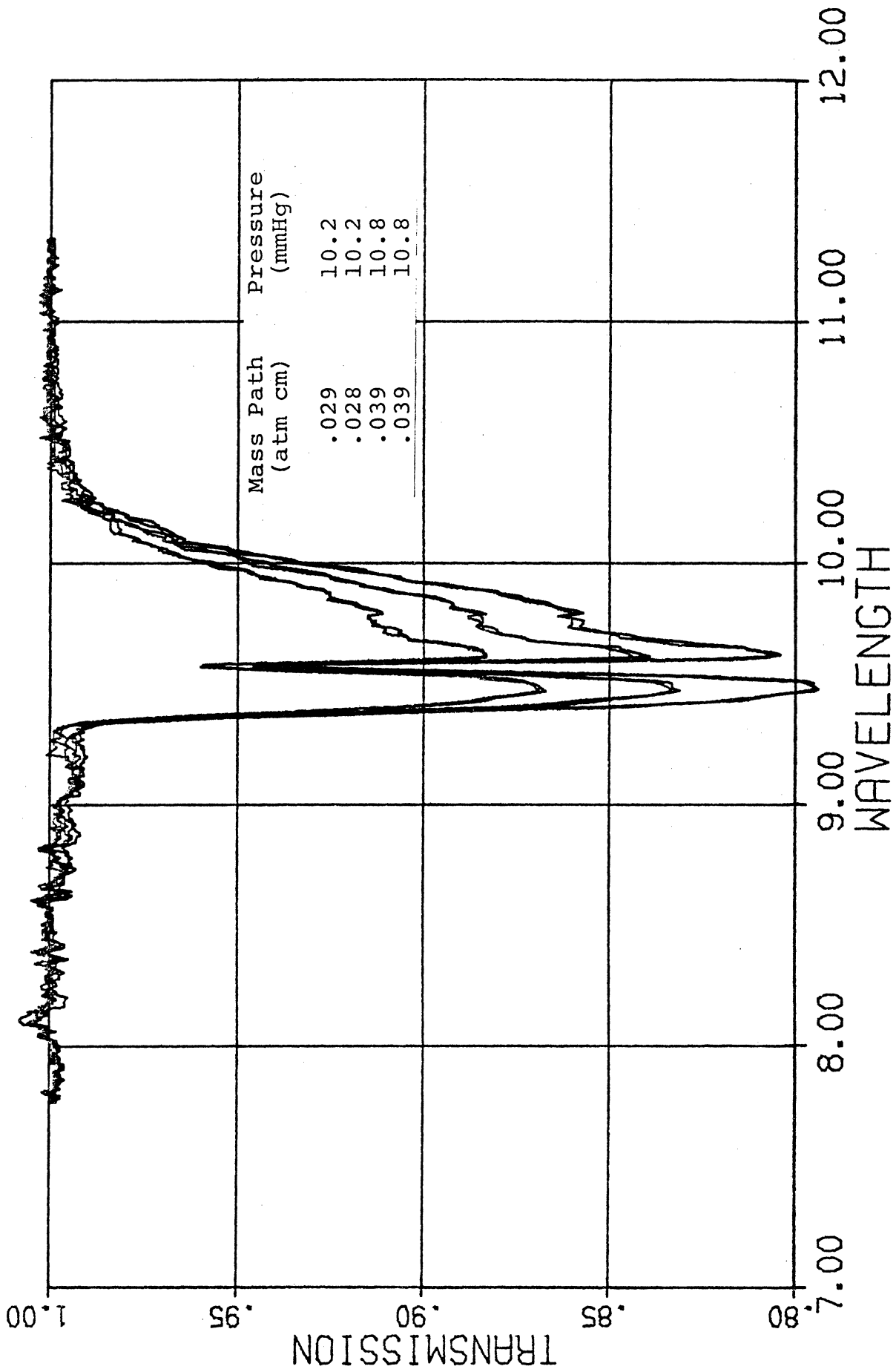


Fig. 4.3.7. Transmission profiles for 9.6 μ m ν_3 ozone band.

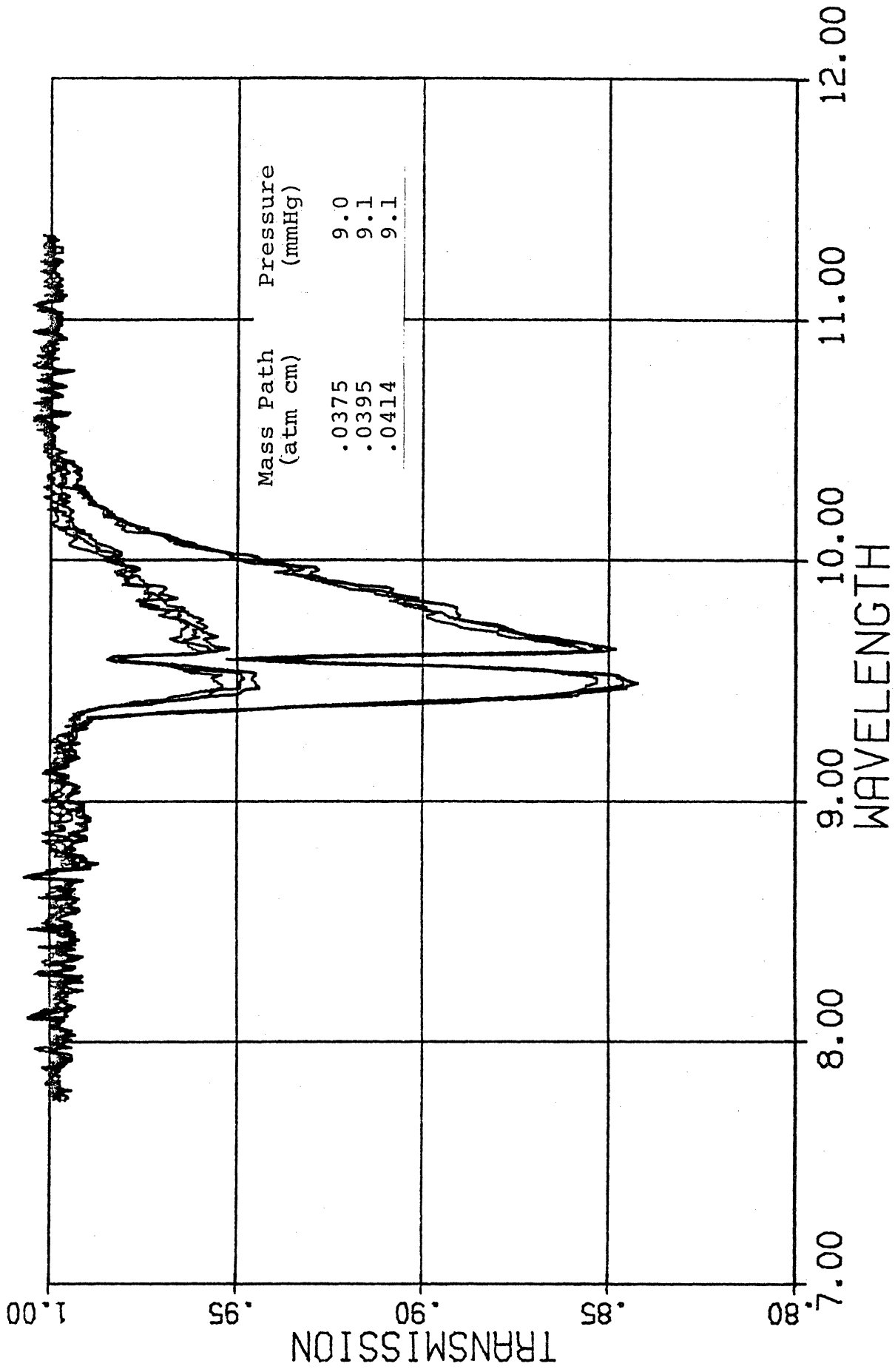


Fig. 4.3.8. Transmission profiles for $9.6\mu\text{m } \nu_3$ ozone band.

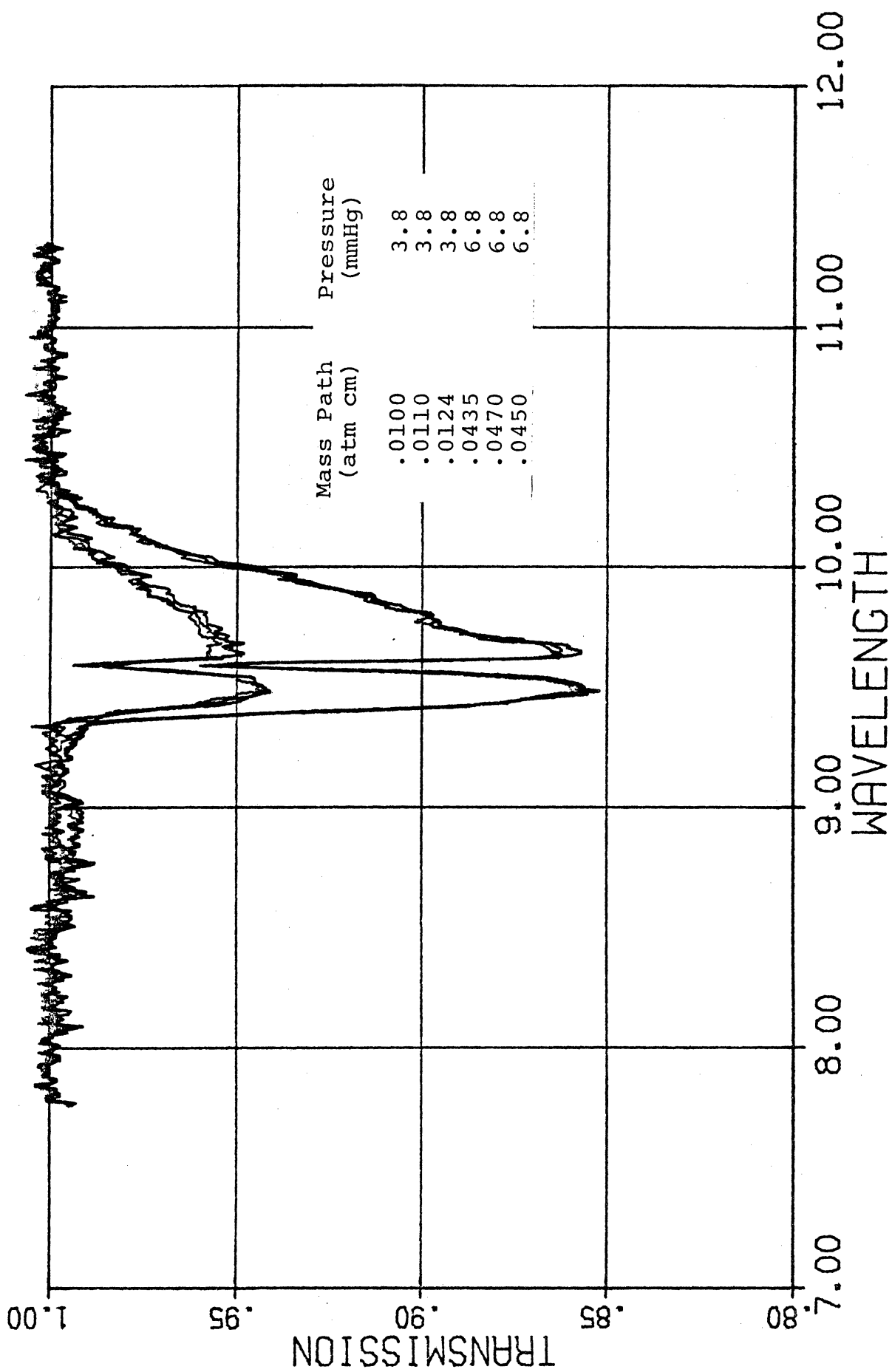


Fig. 4.3.9. Transmission profiles for $9.6\mu\text{m } \nu_3$ ozone band.

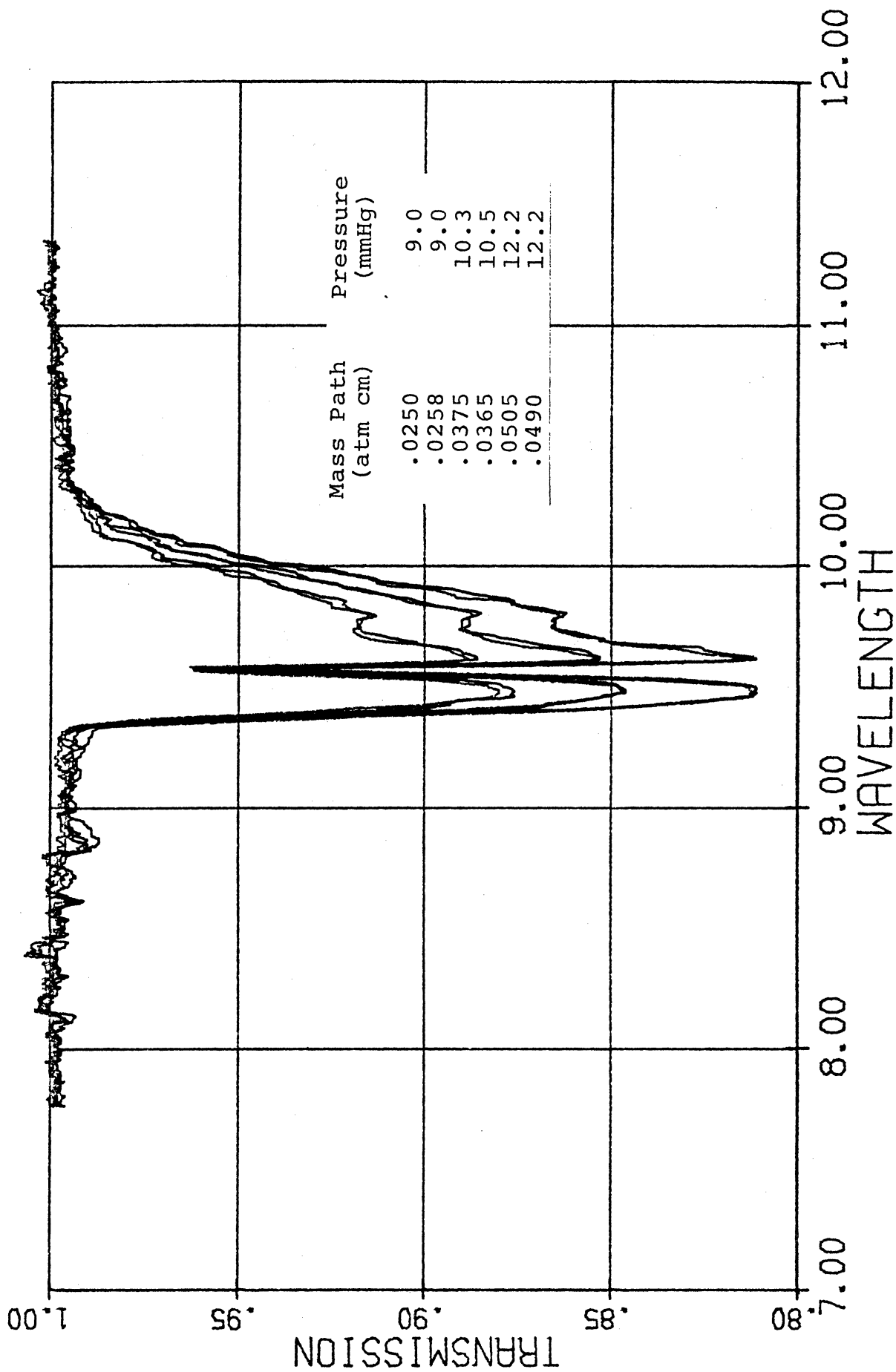


Fig. 4.3.10. Transmission profiles for $9.6\mu\text{m } \nu_3$ ozone band.

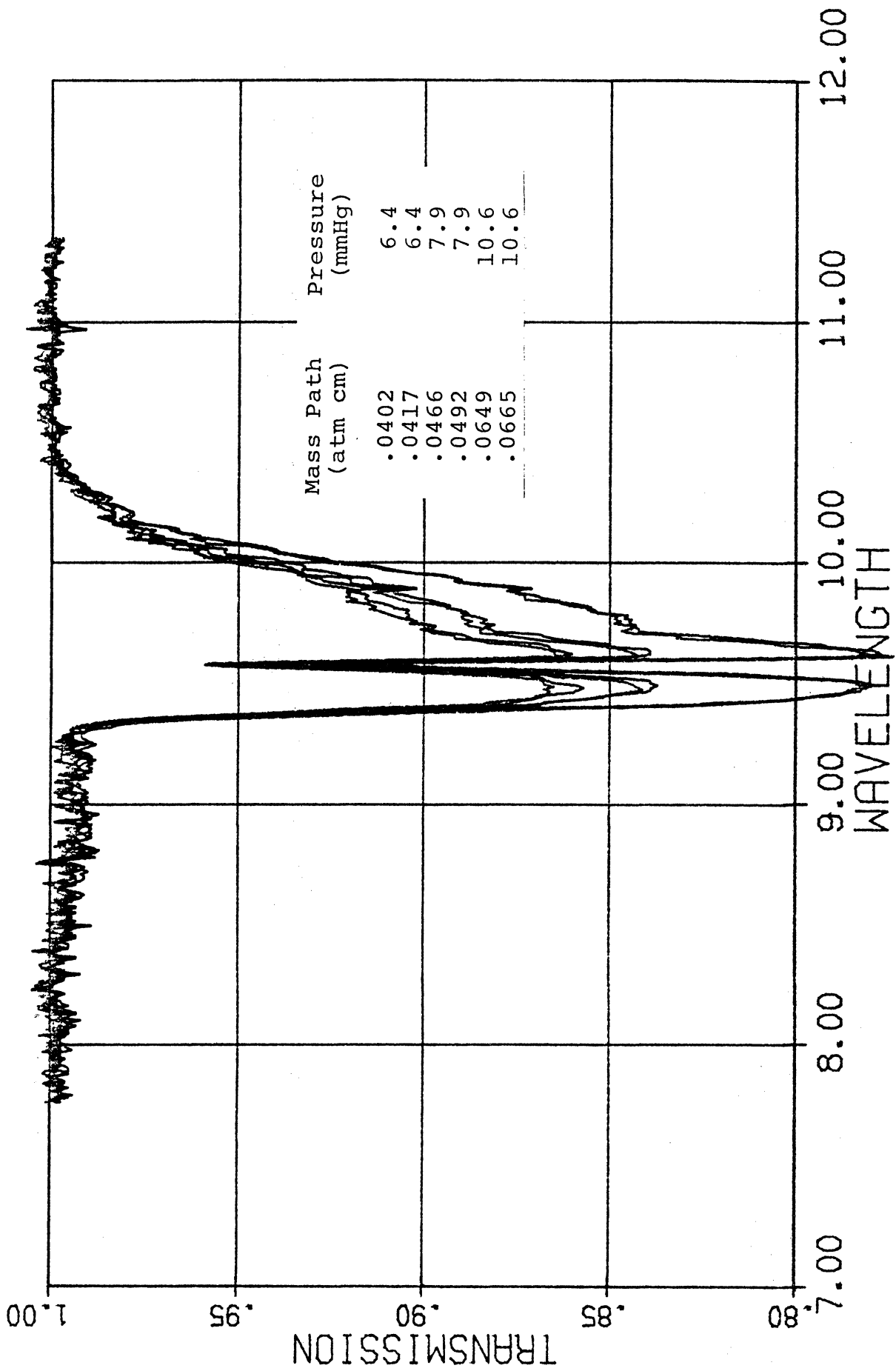


Fig. 4.3.11. Transmission profiles for $9.6\mu\text{m } \nu_3$ ozone band.

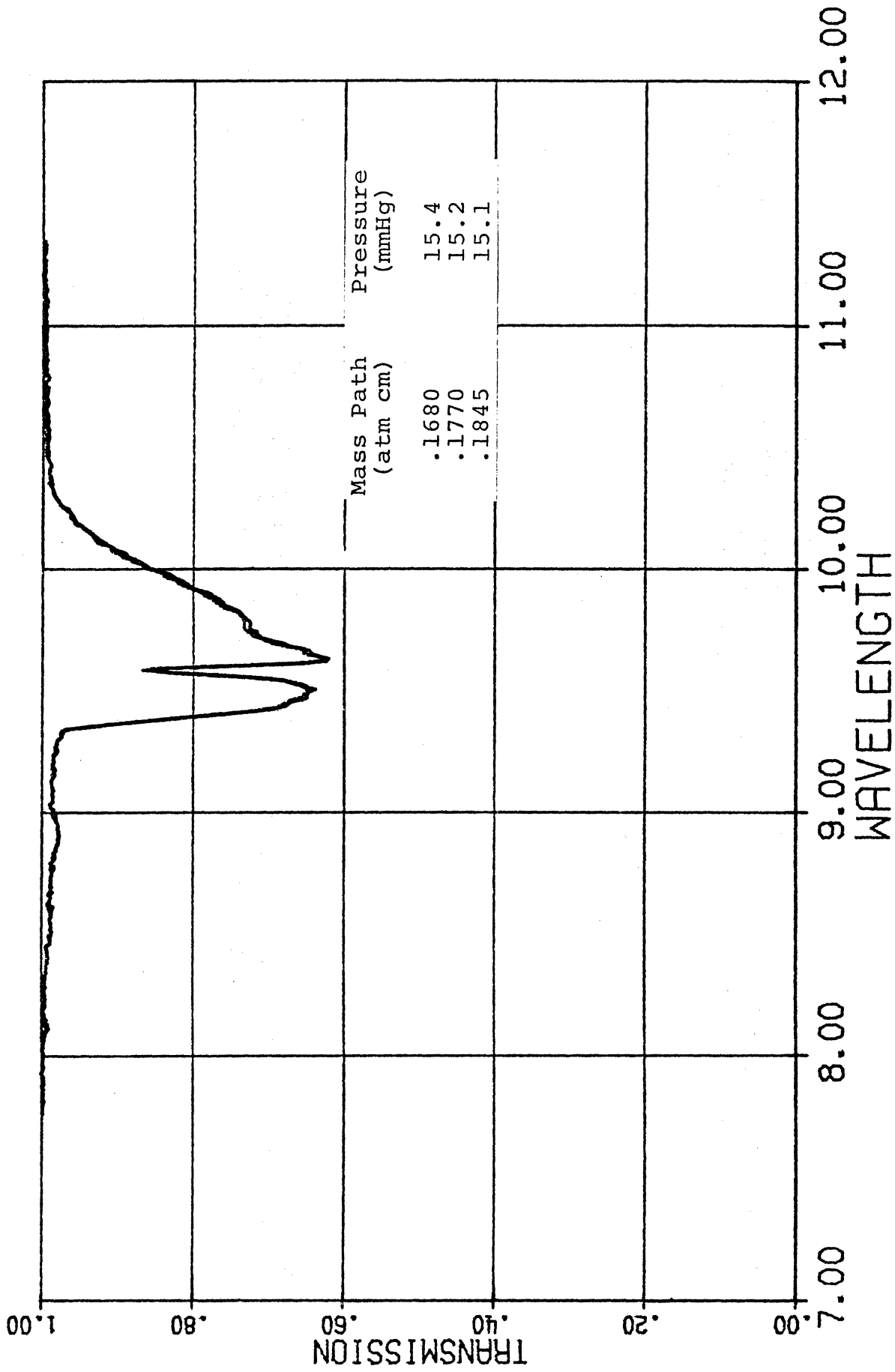


Fig. 4.3.12. Transmission profiles for $9.6\mu\text{m } \nu_3$ ozone band.

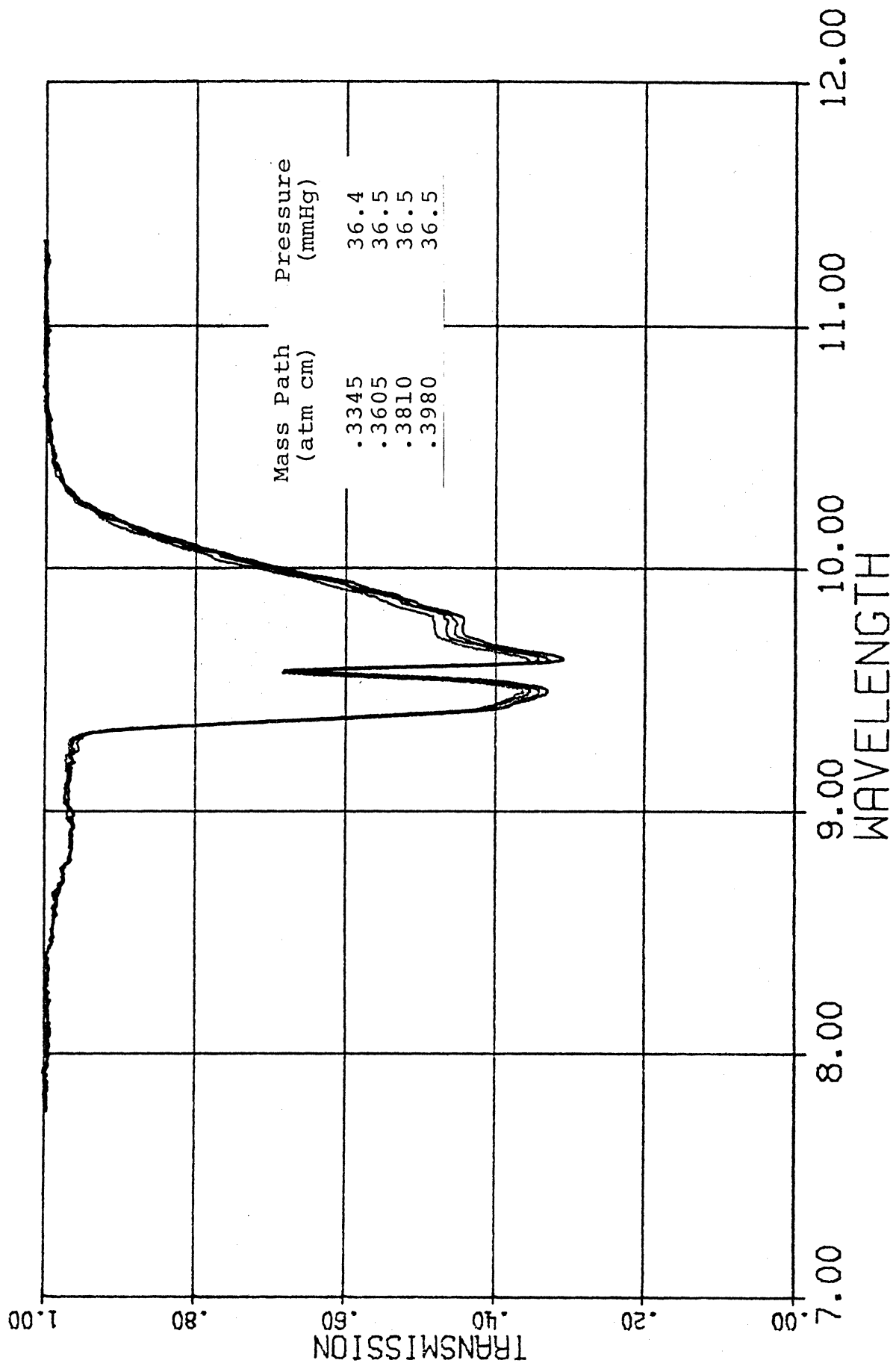


Fig. 4.3.13. Transmission profiles for $9.6\mu\text{m } \nu_3$ ozone band.

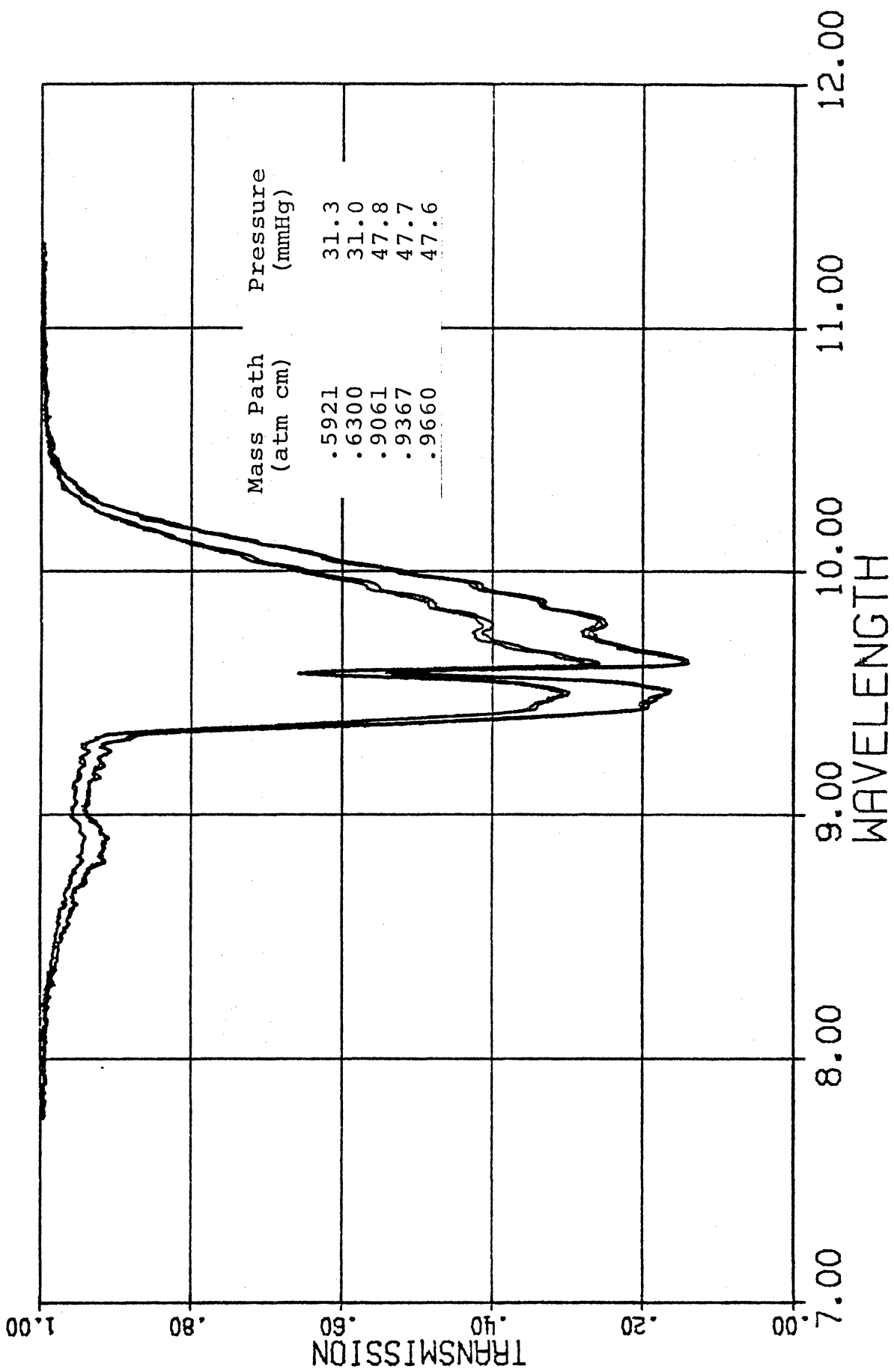


Fig. 4.3.14. Transmission profiles for $9.6\mu\text{m } \nu_3$ ozone band.

TABLE 4.4.1

Low temperature absorptivity measurements for the ν_3 ozone band. * refers to the 2967 Å uv line, all others to the 2536 Å line.

mass path (atm cm)	pressure (mm Hg)	temperature (°C)	Absorptivity (cm ⁻¹)
.0085	8.1	-8	4.81
.0085	10.2	-8	4.83
.0148	13.7	-8	7.85
.0148	14.8	-7	8.04
.0164	5.4	-11	3.60
.0235	18.6	-8	11.30
.0233	20.3	-7	11.51
.0282	8.0	-11	6.05
.0280	8.2	-11	6.21
.0393	5.9	-8	6.96*
.0397	5.7	-9	6.91*
.0684	9.0	-8	11.18*
.0695	8.7	-9	10.95*
.0740	8.1	-10	11.22*
.0746	8.0	-10	11.31*
.1138	10.9	-12	15.48*
.1164	10.7	-11	15.36*
.1346	9.3	-7	16.62*
.1404	9.1	-7	16.15*
.3390	37.4	-8	38.66*
.3501	37.5	-8	38.89*

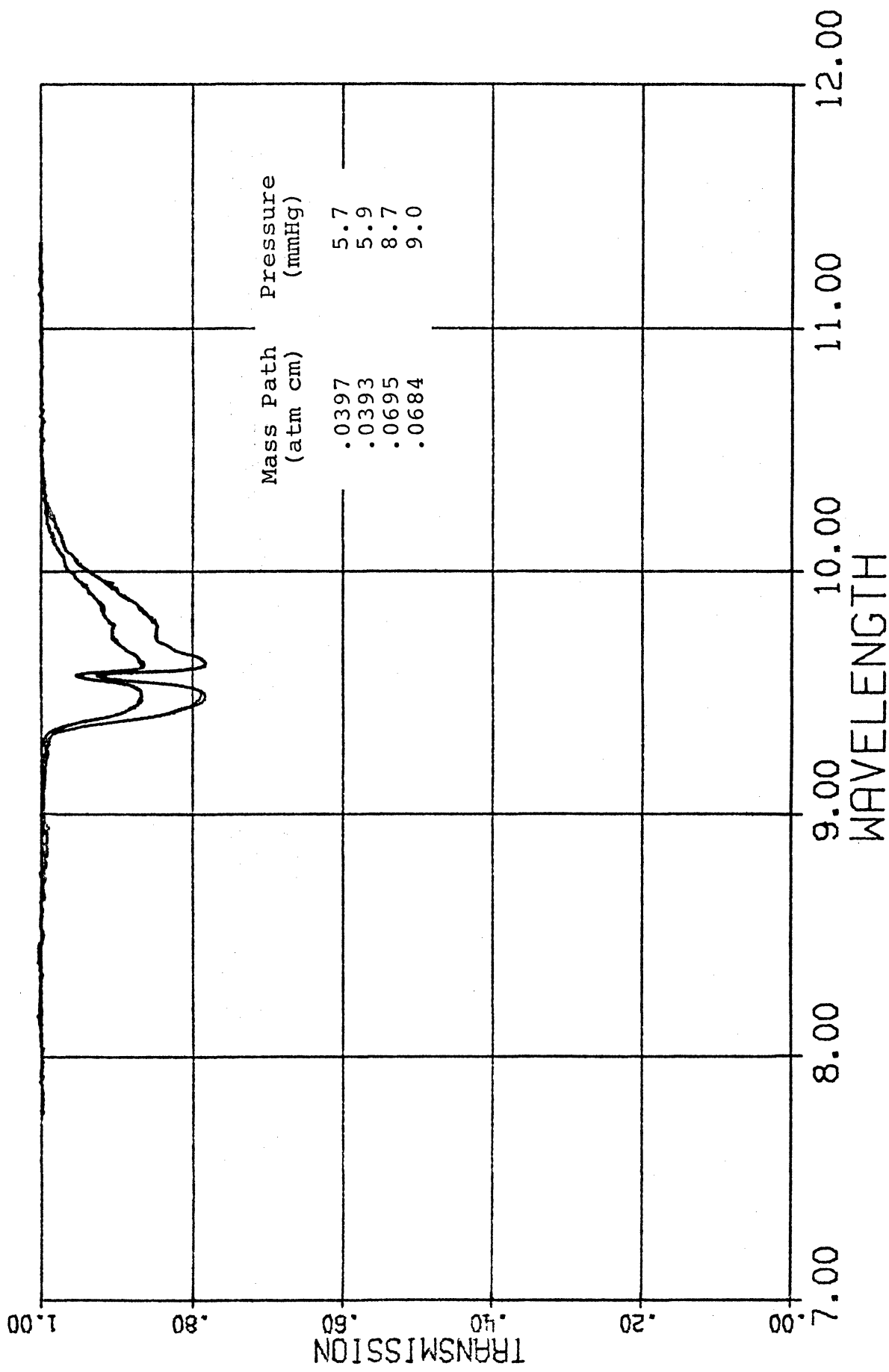


Fig. 4.4.1. Low temperature transmission profiles for $9.6\mu\text{m } \nu_3$ ozone band.

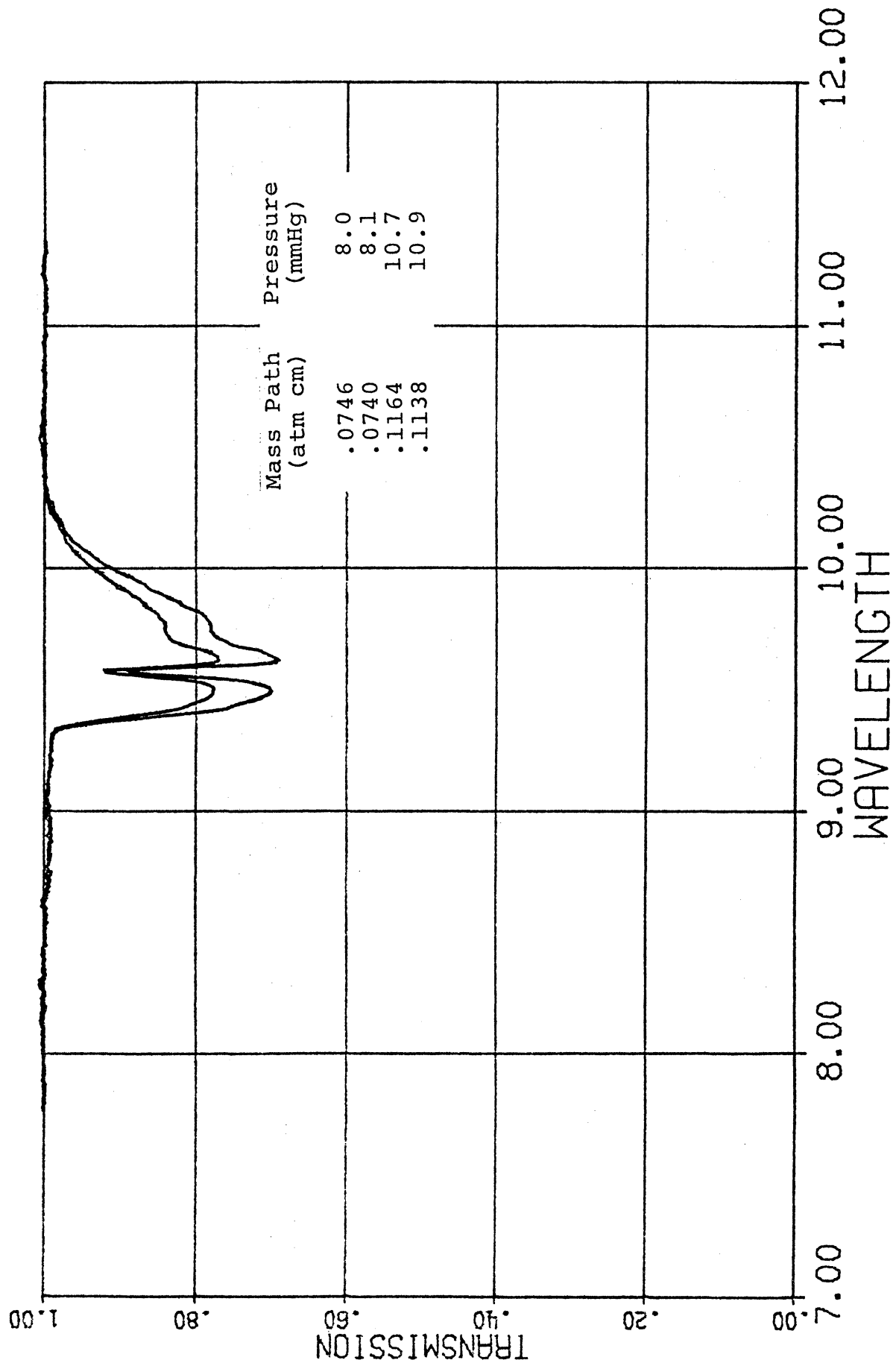


Fig. 4.4.2. Low temperature transmission profiles for the $9.6\mu\text{m } \nu_3$ ozone band.

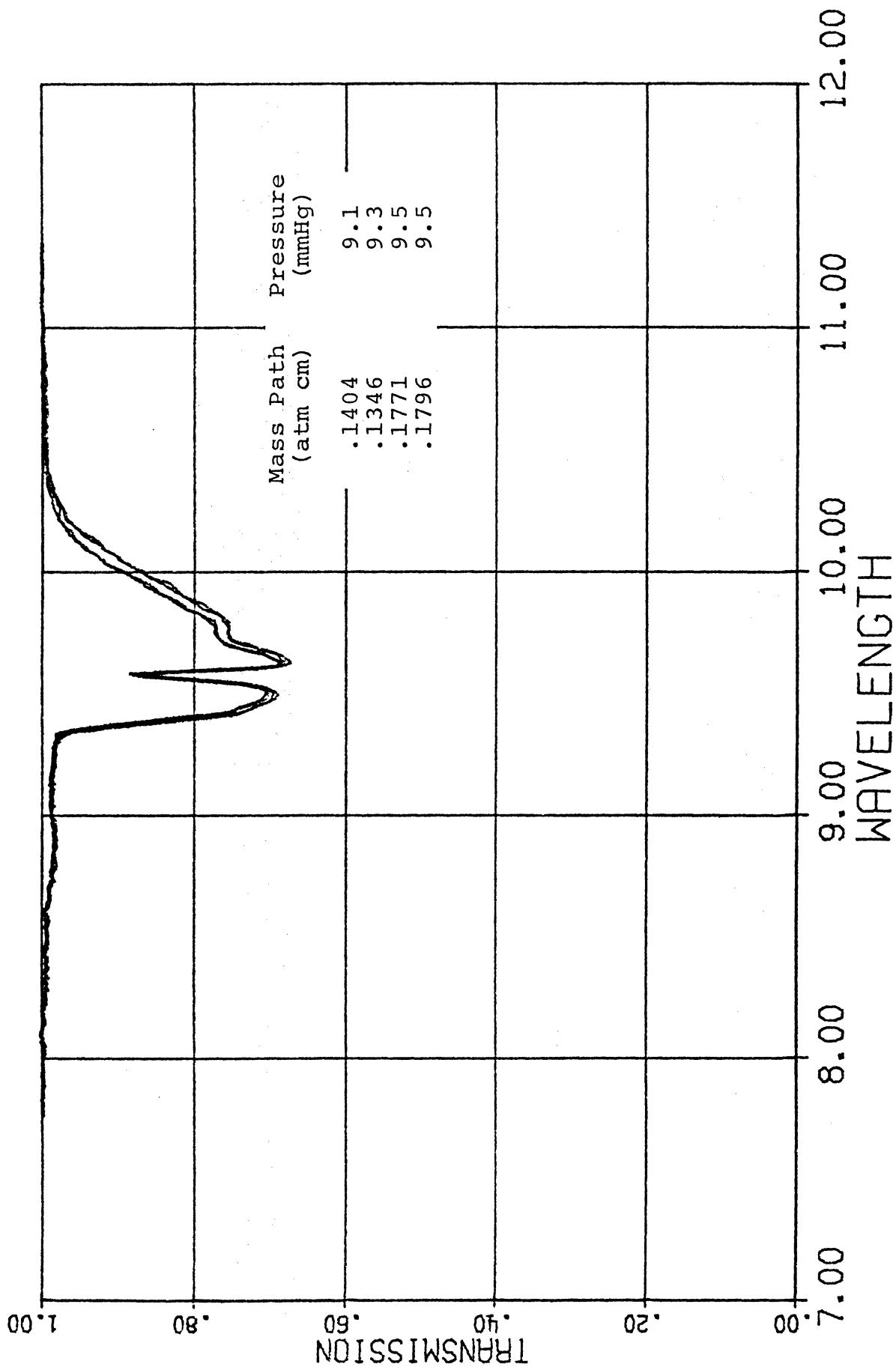


Fig. 4.4.3. Low temperature transmission profiles for the $9.6\mu\text{m } \nu_3$ ozone band.

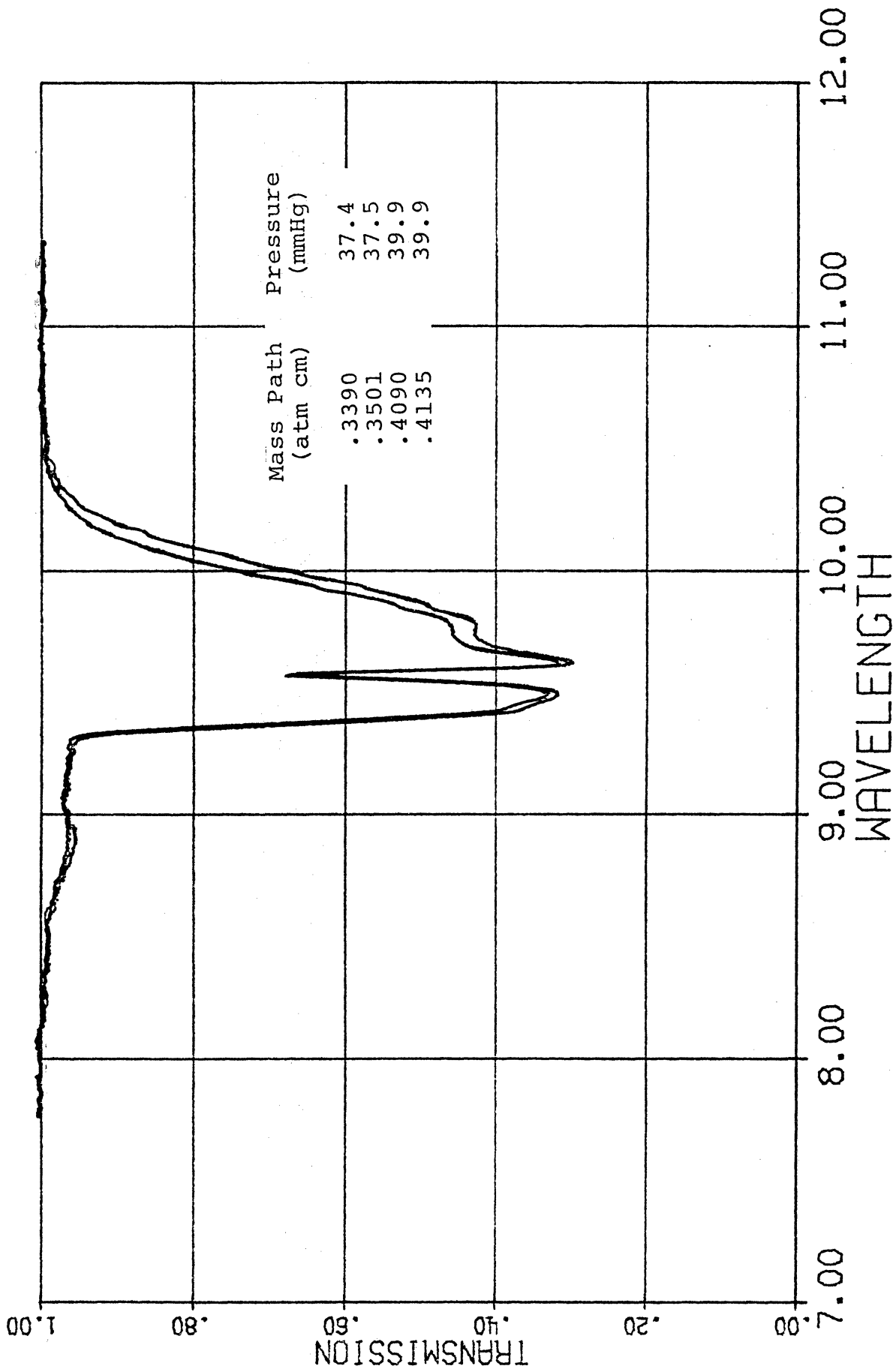


Fig. 4.4.4. Low temperature transmission profiles for the $9.6\mu\text{m } \nu_3$ ozone band.

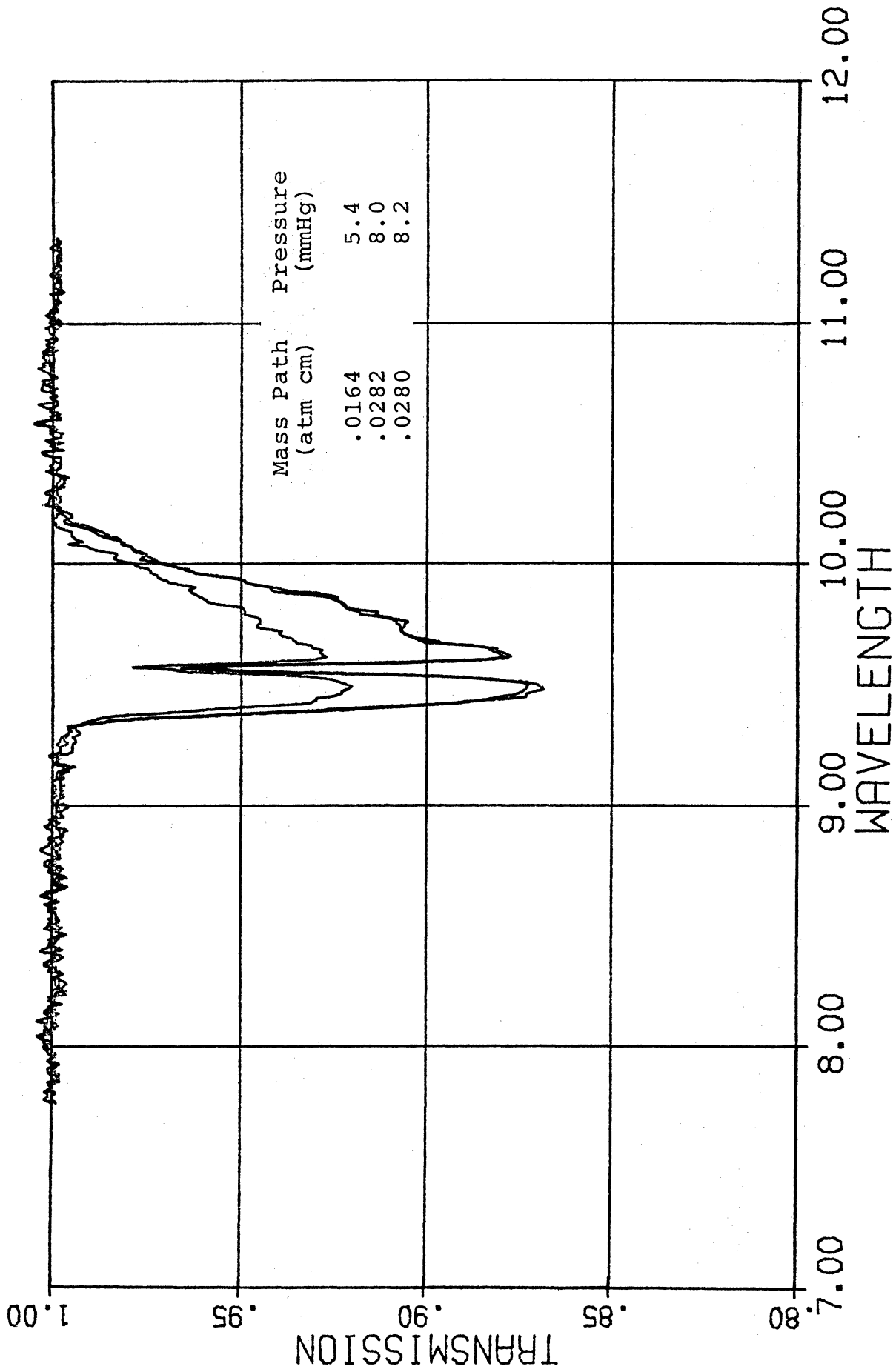


Fig. 4.4.5. Low temperature transmission profiles for the $9.6\mu\text{m } \nu_3$ ozone band.

A comparison of these low temperature measurements with those made at room temperature is difficult since the precise mass paths and pressures could not be duplicated. However, an indication of the differences in transmission for room temperature (~27 C) and reduced temperatures (~-10 C) can be made by comparing Figs 4.3.7 and 4.4.5 for the mass paths and pressures of approximately 0.03atm-cm and 10 mmHg respectively. Note that near 10 μ the low temperature results give a larger transmissivity than those measurements made at room temperature, while nearer band center, e.g. about 9.75 μ , the reverse is true. The difference in transmission is about 1% in both cases which is near the limit of resolution of our measurements, however the difference is not random.

These results are consistent with the theoretical interpretation. The expression for the line strength S at some temperature T can be written,

$$S(T) = S(T_0) \left(\frac{T_0}{T} \right)^{3/2} \exp \left[-1.439 E \left(\frac{1}{T} - \frac{1}{T_0} \right) \right]$$

where $S(T_0)$ is the line strength for some temperature T_0 , and E is the energy in wavenumber units for the lower state energy level. Now for a given transition, i.e. E value, the temperature corresponding to the maximum value of line strength can be found by maximizing the above equation. The result is $T_{\max} = 0.96 E$. The average E values for 5 cm^{-1} spectral intervals centered about 9.75 and 10 μm can be evaluated from the

data of Clough and Kneizys (1965). The results are 747cm^{-1} for the interval centered at $10\mu\text{m}$ and 235cm^{-1} for the interval at $9.75\mu\text{m}$. These values correspond to temperatures of 717°K and 226°K respectively. Thus for a given mass path, as the temperature decreases from about 300°K to 265°K , the temperatures used for our measurements, the line strength in the $10\mu\text{m}$ region decreases so that the transmission increases, while in the $9.75\mu\text{m}$ region, the line strength increases, or the transmission should decrease. This variation is in agreement with our measurements.

To compare the difference in transmission at room temperature (27°C) and reduced temperature (-10°C) for the two spectral intervals and the mass path of 0.03atm-cm , we assume a weak line approximation. The variation in transmission $\Delta\tau$ is then,

$$\Delta\tau = - \frac{u\Delta SN}{\delta}$$

where u is the mass path, ΔS the variation in line strength between temperatures of 27°C and 10°C and δ is the width of the spectral interval. N is the number of lines in the interval. The result for the spectral interval at $10\mu\text{m}$ is $\Delta\tau \sim 0.013$ and for the interval at $9.75\mu\text{m}$, $\Delta\tau \sim -0.010$. Thus the variation in transmission for both intervals is approximately 1% in agreement with our measurements.

REFERENCES

- Clough, S.A., and F.X. Kneizys, 1965: Ozone absorption in the 9.0 micron region. AFCRL rept. no. 65-862.
- Goody, R.M., 1964: Atmospheric Radiation, 1 Oxford Univ. Press, London and New York.
- Hearn, A.G., 1961: Proc. Phys.Soc. (London) 78, 932.
- Inn, E.C.Y. and Y.Tanaka, 1953: J. Opt. Soc. Am., 43, 870.
- Kuhn, W.R. and J. London, 1969: Infrared radiative cooling in the middle atmosphere. J. Atmos. Sci., 26, 189-204.
- Mateer, C.L. D.F. Heath and A.J. Krueger, 1971: Estimation of total ozone from satellite measurements of back scattered ultraviolet earth radiance. J. Atmos. Sci., 28, 1307-1311.
- McCaa, D.J. and J.H. Shaw, 1968: The infrared spectrum of ozone. J. Mol. Spectrosc. 25, 374-397.
- Ny, Tsi-Ze and S.P. Choong, 1933: Chinese J. Phys., 1, pp. 38-50.
- Plass, G.N., 1960: Useful representations for measurements of spectral band absorption. J. Opt. Soc. Amer. 50, 868-875.
- Vigroux, E., 1953: Ann.de Phys., 3, pp. 709-762.
- Walshaw, C.D., 1957: Integrated absorption by the 9.6 μ band of ozone. Quart. J. Roy. Meteor. Soc., 83, 315-321.
- Walshaw, C.D., 1954: An experimental investigation of 9.6 μ band of ozone; dissertation, Cambridge Univ.
- Young, C., and R.H.L. Bunner, 1974: Absorption of carbon dioxide 9.4 μ m laser radiation by ozone, Applied Optics, 13, 1438-1443.

UNIVERSITY OF MICHIGAN



3 9015 03527 0068